J. Fluid Mech. (1996), vol. 315, pp. 317–344

Multi-mode resonances in fluids

By H. OCKENDON, J. R. OCKENDON AND D. D. WATERHOUSE

Mathematical Institute, University of Oxford, 24-29 St. Giles', Oxford, OX1 3LB, UK

(Received 21 September 1995 and in revised form 27 January 1996)

When a lightly damped fluid resonator is forced near its fundamental frequency, the most usual response is one in which the fluid oscillates in the corresponding eigenmode with an amplitude response similar to that of a Duffing oscillator. Examples are the sloshing of a horizontally oscillated tank or acoustic oscillations in a resonator of general shape. However, multiple eigenmodes can be excited if the spectrum is either commensurate or degenerate and both acoustic resonance and the sloshing of shallow water in a nearly square container exemplify both these exceptional cases. In this paper we investigate how the response of such systems depends on geometry and dispersion.

1. Introduction

1.1. *Preamble*

When any mechanical system is subjected to a small oscillatory driving force, a resonant response will occur whenever the difference between the frequency of the driving force and a natural frequency, usually the fundamental, tends to zero. This frequency difference is called the detuning. In systems with several degrees of freedom, the response can be quite a complicated function of the detuning, typically taking the form of coupled damped oscillators when dissipation limits the amplitude or of coupled Duffing oscillators when nonlinearity is the limiting mechanism. For continuous systems such as fluids, the situation is further complicated by the dependence on the geometry. However, all resonances, whether in finite- or infinite-dimensional systems, can be attacked by exploiting the smallness of the forcing amplitude and the detuning. Our aim in this paper is to use asymptotic methods to shed light on some interesting cases of fluid resonance that are primarily limited by nonlinearity and have received little attention theoretically or experimentally. Because the subject of fluid resonances has quite a complicated history, we can only put our work in context by subjecting the reader to this regrettably lengthy introduction.

Those fluid resonances that have received most theoretical attention concern

(*a*) the sloshing of liquids in a horizontally oscillated, rectangular tank;

(*b*) one-dimensional, radially symmetric or spherically symmetric acoustic oscillations in a closed resonator.

These two situations can be related to each other when the liquid in (*a*) is sufficiently shallow. In all the cases that have been considered, the resonant response is best classified according to the distribution of the natural frequencies of the system. Thus, in case (*a*), whenever the liquid depth is comparable to or greater than the horizontal dimensions of the resonator, implying that the system usually only contains

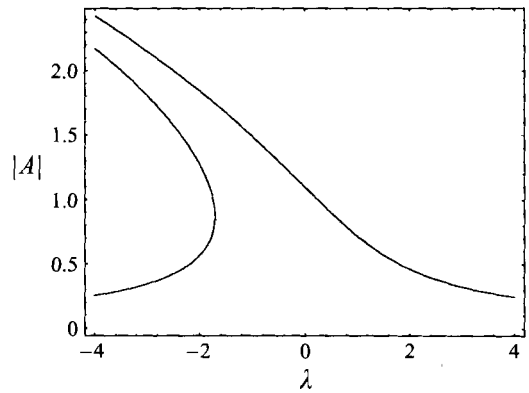

FIGURE 1. Duffing-type response showing amplitude against frequency for soft-spring behaviour.

simple non-commensurate eigenvalues, the undamped periodic resonant response is analogous to that of the classical Duffing oscillator

$$\ddot{x} + (1 + \lambda\varepsilon^{2/3})x + x^3 = \varepsilon\cos t, \quad \varepsilon \ll 1, \tag{1.1a}$$

for which

$$x \sim \varepsilon^{1/3} A\cos t + \cdots \quad \text{where} \quad \lambda A + \tfrac{3}{4}A^3 = 1. \tag{1.1b}$$

Here λ is the detuning and ε is the forcing amplitude, and the soft-spring response ($\varepsilon > 0$) is illustrated in figure 1. This 'deep-water' result was obtained in the pioneering work of Moiseyev (1958). It describes the simplest resonant behaviour that a fluid can exhibit, because the non-commensurability of the spectrum means that the lowest-order response, although nonlinear in amplitude, is proportional to a single normal mode. This scenario also encompasses acoustic resonance in a closed resonator as in (*b*) above when the geometry is such that the spectrum is non-commensurate; indeed, for such oscillations in a sphere or in a cylindrical wedge, the nonlinear response has been shown to comprise only a single mode by Chester (1991) and Ellermeier (1994) respectively.

However, the response is quite different when any of the natural frequencies are commensurate or degenerate (i.e. with more than one corresponding normal mode) and conceptually, the next level of complexity occurs when there are just a finite number of commensurate, simple eigenvalues. Then, as shown in Can & Askar (1990), Peake (1993) and Waterhouse (1995), the resonant response is analogous to that of a coupled system of Duffing oscillators. As discussed in Ockendon *et al.* (1993), a similar response in the form of a finite combination of modes may still occur to lowest order even when there are an infinite number of commensurate eigenvalues, just as long as there are also some non-commensurate ones as well; this happens because nonlinearities in the field equations can prevent higher eigenmodes from being excited, despite their frequencies being commensurate with the driving frequency. However, the most extreme case of commensurability occurs in (*b*) above when the resonator is a cylinder such as an organ pipe. As shown in the original paper of Chester (1964), the fact that the spectrum now comprises the integers means that when the gas is oscillated in the direction of the axis of the cylinder near the fundamental frequency, *all* the higher modes can be simultaneously excited. These modes form a complete set and hence much more complicated waveforms can appear than with finite combinations of normal modes. In particular there is the possibility of discontinuous solutions that

include shock waves when the detuning λ is sufficiently small. Indeed this is apparent from the solution of 'Chester's equation' (Chester 1964, 1968)

$$\lambda f'' + (\gamma + 1) f' f'' = -\frac{\sin t}{\pi}, \tag{1.2}$$

which describes the pressure, $f'(t)$, at one end of the resonator, γ being the ratio of specific heats.

This leaves one other class of problems, namely those in which the spectrum has some degenerate natural frequencies with independent corresponding eigenmodes, and this is the situation with which we will mainly be concerned in this paper. The effect of such degeneracy is relatively easy to describe for case (*a*) above and we will see in §1.3 how it engenders strong multi-dimensional responses in systems that are very nearly one-dimensional. However, the situation is more complicated when the spectrum is also nearly commensurate and, in order to encompass this situation, we will find it most convenient to describe our results in terms of the solution of a canonical nonlinear, non-dispersive scalar wave equation that will apply to both acoustic and shallow sloshing resonances. We will describe this equation later in the introduction and the relevance of its solutions to case (*a*) will then be explained by modifying its predictions to account for dispersion.†

Most of the remainder of this introduction will be devoted to describing the models within which we propose to study multi-dimensional degenerate resonance. We will assume throughout that the damping is such as to allow us to only consider periodic responses that are synchronous with the forcing. Also, from the start, we will work with the dimensionless variables used in Ockendon & Ockendon (1973) and Ockendon *et al.* (1993), and the crucial parameters ε, λ and ν will always be associated with the forcing amplitude, the detuning and the geometrical imperfections respectively.

1.2. *Uni-modal response*

1.2.1. *Deep water sloshing*

The analysis of this case is predicated on the fact that the scaling needed to obtain the solution (1.1), as $\varepsilon \to 0$, is $x \sim O(\varepsilon^{1/3})$ with the detuning being of $O(\varepsilon^{2/3})$. Now the sloshing problem for irrotational motion in a horizontally oscillated tank is

$$\nabla^2 \phi = 0, \tag{1.3a}$$

with the conditions

$$\phi_z = \eta_t + \varepsilon \left(\phi_x \eta_x + \phi_y \eta_y\right), \tag{1.3b}$$

$$\eta + (1 + \lambda_0) \tanh h \left[\phi_t + \tfrac{1}{2}\varepsilon \left({\phi_x}^2 + {\phi_y}^2 + {\phi_z}^2\right)\right] = 0, \tag{1.3c}$$

on the free surface $z = \eta$. Here, $\varepsilon \ll 1$ is the ratio of the amplitude of the forcing to a typical tank dimension L, the dimensional undisturbed water depth is hL, the dimensional velocity potential is $\varepsilon\omega L^2\phi$, the dimensional surface elevation is $\varepsilon L\eta$ and the tank is oscillated at a frequency ω near its fundamental frequency ω_0 so that

$$\omega^2 = (1 + \lambda_0)\omega_0^2, \tag{1.4}$$

† This bridging between dispersive and non-dispersive resonances has been discussed for non-degenerate spectra by Chester (1968), Ockendon & Ockendon (1973) and Ockendon, Ockendon & Johnson (1986).

and the normal velocity ϕ_n is proportional to $\sin t$ on the walls of the tank. For uniqueness, we also need to prescribe the mean elevation so that

$$\int_D \eta \, dx \, dy = 0, \tag{1.5}$$

where D is the domain of the free surface. We now follow the scalings suggested by Moiseyev (1958) and consider the regime $\lambda_0 = \lambda_d \varepsilon^{2/3}$ ($\lambda_d \sim O(1)$, the suffix d denoting deep water) and employ the expansions

$$\phi \sim \varepsilon^{-2/3}\phi_0 + \varepsilon^{-1/3}\phi_1 + \phi_2 + \cdots, \tag{1.6a}$$

$$\eta \sim \varepsilon^{-2/3}\eta_0 + \varepsilon^{-1/3}\eta_1 + \eta_2 + \cdots, \tag{1.6b}$$

to find that ϕ_0 is just A times the normalized fundamental eigenmode proportional to $\sin(t + \theta)$, where θ is the phase shift. Then, by applying the Fredholm Alternative to the problem for ϕ_2, we find that $\sin\theta = 0$ and

$$\alpha\lambda_d A + \beta A^3 = \cos\theta, \tag{1.7}$$

for some constants α and β, where the phase $\theta = 0$ or π is chosen so that $A > 0$, i.e. the response is qualitatively as in (1.1).

We will subsequently be especially interested in the case when the tank is a cuboid of non-dimensional depth h, length π and breadth b for which $\omega_0^2 = (g/L)\tanh h$ and

$$\phi_x = \sin t \quad \text{on} \quad x = -\varepsilon\cos t, \pi - \varepsilon\cos t, \tag{1.8a}$$

$$\phi_z = 0 \quad \text{on} \quad z = -h, \tag{1.8b}$$

$$\phi_y = 0 \quad \text{on} \quad y = 0, b, \tag{1.8c}$$

and in this case

$$\phi_0 = A\cos x \cosh(z + h)\sin(t + \theta), \tag{1.9}$$

$\alpha = \pi/(4\cosh h)$, $\beta = (\pi/4)\coth h H(h)$ and $H(h)$ is given by (A 1) in the Appendix.†

1.2.2. *Acoustic resonators*

As discussed in Ockendon *et al.* (1993), a suitable reduction of the equations of two-dimensional gas dynamics leads to the prototype model for this class of resonators as the nonlinear wave equation

$$\varphi_{xx} + \varphi_{yy} - \varphi_{tt} - \lambda_0\varphi_{tt} = \varepsilon\left[2\varphi_x\varphi_{xt} + 2\varphi_y\varphi_{yt} + (\gamma - 1)\varphi_t(\varphi_{xx} + \varphi_{yy})\right], \tag{1.10}$$

where we are given Neumann data as in (1.8*a*). The non-dimensionalization and the parameters ε, λ_0 are as before, and γ is the ratio of specific heats. Thus we can again adopt the asymptotic expansions $\varphi \sim \varepsilon^{-2/3}\varphi_0 + \varepsilon^{-1/3}\phi_1 + \phi_2 + \cdots$, $\lambda_0 = \varepsilon^{2/3}\lambda_a$ and find that φ_0 is the fundamental eigenmode with an amplitude satisfying an equation identical to (1.7) with λ_d replaced by λ_a. Indeed, such a statement could be made about any weakly nonlinear wave equation with quadratic nonlinearity. However, these scalings cannot be applied uniformly in a variety of different limits. In particular, (1.7) will not be uniformly valid when the shape of the tank or resonator is close to one in which the lowest eigenfrequency is degenerate or is close to one with a commensurate spectrum. We now consider these cases in turn.

† This response exhibits a change from soft to hard spring behaviour around $h \simeq 1.06$, causing H to change sign. The behaviour near this critical depth has been discussed by Waterhouse (1994).

1.3. *Multi-dimensional responses*

1.3.1. *Deep water sloshing*

An obvious configuration in which to study sloshing when the fundamental is nearly degenerate is the nearly square tank problem (1.3), (1.5), (1.8) when b is close to π. If b is any constant not a multiple of π and we allow the breadth of the tank to vary slightly with x, we still retrieve (1.9) to lowest order and the solution is virtually one-dimensional. However, when we replace (1.8c) by

$$\phi_y = \nu_0 \pi \phi_x a'(x) \quad \text{on} \quad y = \pi\,[1 + \nu_0 a(x)]\,, \tag{1.11}$$

where ν_0 is a small parameter characterizing the breadth variations, we find that a new phenomenon occurs when $\nu_0 = \nu_d \varepsilon^{2/3}$ ($\nu_d \sim O(1)$). Now ϕ_0 has to be a linear combination of the phase-shifted eigenmodes

$$\phi_0 = (A \cos x \sin(t + \theta_1) + B \cos y \sin(t + \theta_2)) \cosh(z + h). \tag{1.12}$$

The all-important criterion that determines the amplitudes A and B and the phases θ_i is again found by solving for ϕ_1 and then insisting that the problem for ϕ_2 has a solution with period 2π in t and it can only be satisfied when $B \neq 0$. Indeed, as shown in Waterhouse (1995), the Fredholm Alternative implies the solvability conditions $\sin\theta_1 = \sin\theta_2 = 0$ and

$$\frac{4}{\pi} \tanh h = [\nu_d L(h) A + \lambda_d A \sinh h + H(h) A^3 + J(h) A B^2] \cos\theta_1 + \nu_d K(h) B \cos\theta_2, \tag{1.13a}$$

$$0 = [\nu_d M(h) B + \lambda_d B \sinh h + H(h) B^3 + J(h) B A^2] \cos\theta_2 + \nu_d K(h) A \cos\theta_1, \tag{1.13b}$$

where the coefficients in (1.13) are given in the Appendix and $\theta_i = 0$ or π are chosen as shown in figure 2, so that $A, B > 0$. We can check this by recalling that when the tank breadth is not commensurate with its length, the leading-order transverse mode is no longer resonant and we should return to (1.9). This can be seen by letting the average of the geometric imperfection tend to infinity so that, from (A5) and (1.13b), we find $B \to 0$ and hence A satisfies an equation similar to (1.7). We note that we can interpret (1.13) in terms of a response diagram as in figure 2, where we have considered a fixed geometric variation ($\nu_d = 2$) and shown, in the case $a'(x) = 2x$ (which will later be seen to be a useful special case) and $h = 1.5$, the variation in amplitude as the detuning, λ_d, varies. Similar response pictures can be found for other values of ν_d and other $a(x)$. This picture contrasts with figure 1 in that that there are now two branches due to the interaction between the two modes, reflecting the degeneracy of the first eigenvalue. For ν_d non-zero, the perturbed eigenvalues are at

$$\lambda_d = \frac{\nu_d}{2 \sinh h} \left\{ K(h) \pm [L^2(h) + 4K^2(h)]^{1/2} \right\},$$

as reflected in figure 2, where the choice of parameters gives $\lambda_d = 4.6, -5.9$.

The linear coupling terms in (1.13), causing the two distinct branches in figure 2, only arise when the tank breadth is approximately π and $a(x)$ is non-zero; even if we were to oscillate two adjacent vertical walls of the cuboid when either of these conditions is violated, we would simply obtain a superposition of two Duffing-like responses in each direction.

1.3.2. *Acoustic resonators*

It is when we come to consider resonance for problems with spectra that may be *both* degenerate and commensurate that the nonlinear wave equation (1.10) comes

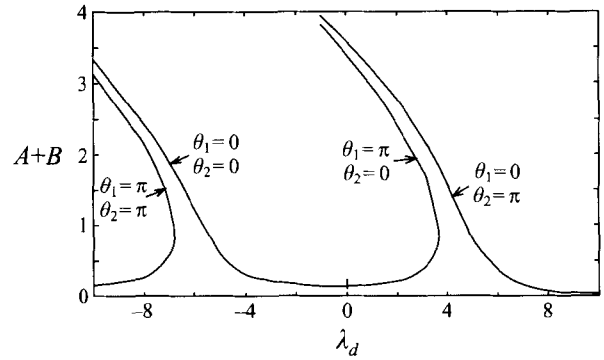

FIGURE 2. Response diagram for deep water when $\nu_d = 2$, $h = 1.5$.

into its own. For, suppose we consider a resonator that is nearly rectangular and forced on one face with an amplitude appropriate to the scalings in §1.2.2. Thus the boundary conditions are

$$\varphi_x = 0 \quad \text{on} \quad x = 0, \tag{1.14a}$$

$$\varphi_x = \sin t \quad \text{on} \quad x = \pi, \tag{1.14b}$$

$$\varphi_y = 0 \quad \text{on} \quad y = 0, \tag{1.14c}$$

$$\varphi_y = \nu_0 \frac{h_0}{L} \varphi_x a'(x) \quad \text{on} \quad y = \frac{h_0}{L}[1 + \nu_0 a(x)], \tag{1.14d}$$

and this corresponds to $\omega_0 = a_0/L$ where $a_0^2 = \gamma p_0/\rho_0$ and p_0 and ρ_0 are the pressure and density in the undisturbed gas. We now see that for $\varepsilon = \nu_0 = 0$, we have a spectrum that not only contains the integers but can also be degenerate when h_0/L is an integer multiple of π. However, whereas for (1.3), (1.5), (1.8) and (1.11) it was easy to retrieve the single mode response (1.9) as we moved away from degeneracy by letting $\nu_d \to \infty$, the dependence of the solution of (1.10), (1.14) on ν_0 is much more subtle as we will see shortly. In fact, the simplest non-trivial case we can consider for $h_0/L = O(1)$ is when $\nu_0 = \nu\varepsilon^{1/2}$ ($\nu \sim O(1)$) so that the imperfection has only a second-order effect. Then we can expand $\varphi \sim \varepsilon^{-1/2}\varphi_0 + \varphi_1 + \cdots$ in the detuning range $\lambda_0 = \lambda\varepsilon^{1/2}$ ($\lambda \sim O(1)$), and, writing $\varphi_0 = A(x, y, t)$ and $\varphi_1 = B(x, y, t)$, the key criterion analogous to (1.13) is that the linear problem for perturbations to the eigensolution satisfying

$$A_{xx} + A_{yy} = A_{tt}, \tag{1.15a}$$

$$A_x = 0 \quad \text{on} \quad x = 0, \pi, \tag{1.15b}$$

$$A_y = 0 \quad \text{on} \quad y = 0, \frac{h_0}{L}, \tag{1.15c}$$

namely

$$B_{xx} + B_{yy} - B_{tt} = \lambda A_{tt} + 2A_x A_{xt} + 2A_y A_{yt} + (\gamma - 1)A_t A_{tt}, \tag{1.16a}$$

$$B_x = 0 \quad \text{on} \quad x = 0, \tag{1.16b}$$

$$B_x = \sin t \quad \text{on} \quad x = \pi, \tag{1.16c}$$

$$B_y = 0 \quad \text{on} \quad y = 0, \tag{1.16d}$$

$$B_y = \nu \frac{h_0}{L}[A_x a'(x) - A_{yy} a(x)] \quad \text{on} \quad y = \frac{h_0}{L}, \tag{1.16e}$$

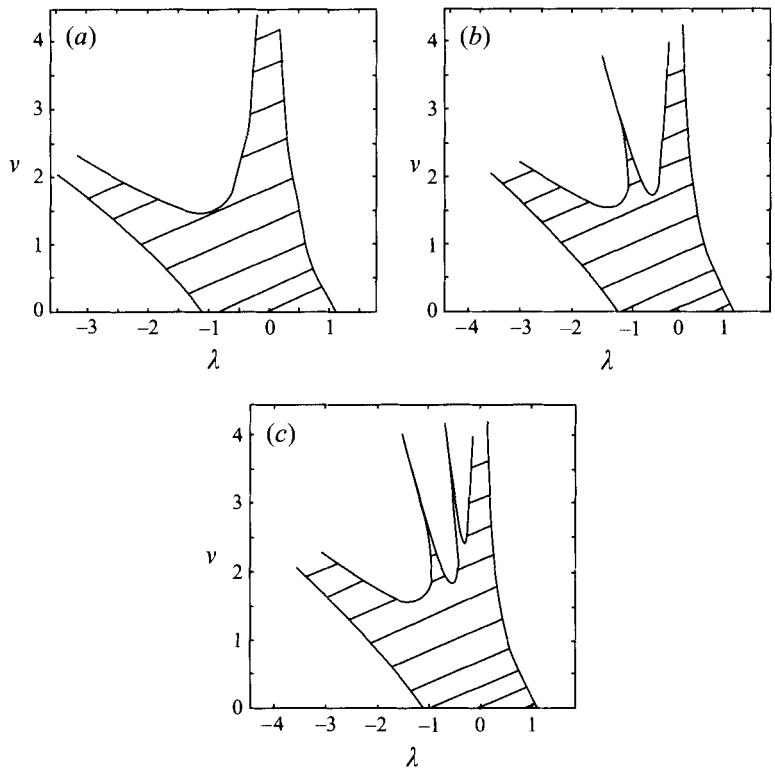

FIGURE 3. 'Shock diagrams' (where shocks occur in the shaded region) for successive approximations to the function $a'(x) = 2x$ for $\gamma = 1.4$. (*a*) $N = 2$, (*b*) $N = 4$, (*c*) $N = 6$.

should have solutions periodic in t with period 2π. We now have the challenging task of using the solvability condition for B in (1.16) to find A and this is our objective in §2; it is only easy to do this in the purely one-dimensional case ($\nu = 0$) when $A = f(t + x) + f(t - x)$ and the solvability condition on (1.16) retrieves (1.2) for the determination of f.

However, as shown in Ockendon *et al.* (1993), there is one parameter regime in which a relatively straightforward asymptotic analysis can be made and that is when h_0/L is small; this situation corresponds to a 'thin' resonator, where the restriction $\nu h_0^2/L^2 \ll 1$ allows the equations (1.10), (1.14) to be integrated across the breadth of the resonator. This leads to a hierarchy of one-dimensional models which show an extreme sensitivity to the size of ν, even though, in general terms, the likelihood of shocks decreases as the cross-sectional area variations, and hence the probable non-commensurability of the spectrum, increases. For these thin resonators the following two parameter regimes emerge in Ockendon *et al.* (1993):

(*a*) $\nu \ll \varepsilon^{-1/2}$. Here, the regime where discontinuous solutions occur is described by 'fingers' in the (λ, ν)-plane within which shocks may be sustained, and the widths of these fingers diminish as ν increases (see Ockendon *et al.* 1993, figure 3, which is similar to figure 3 above which we will refer to as a 'shock diagram'). As in the discussions leading to (1.15), the analytical expression of this statement is only at all easy when $\nu \sim O(1)$ in which case we can expand φ to derive one-dimensional versions of (1.15) and (1.16) and show that $A = f(t + x) + f(t - x)$ where (1.2) is

replaced by

$$\lambda f'' + (\gamma + 1) f' f'' + \frac{1}{\pi} \sin t = \frac{\nu}{2\pi} \int_0^{\pi} [a'(\tau) - a'(\pi - \tau)] f'(t + 2\tau) \mathrm{d}\tau. \tag{1.17}$$

Although (1.17) can only be solved numerically in general, the emergence of narrow shock regimes or fingers as ν increases can be discerned analytically in the special case when $a'(x)$ is linear in x (so that the resonator is parabolic), as described in Ockendon *et al.* (1993). When $a'(x) = 2x$, the right-hand side of (1.17) is $\nu f(t)$ and it is relatively easy to carry out an asymptotic analysis as $\nu \to \infty$. This gives $f \sim \sin t/\pi(\nu + \lambda)$ unless $-\nu/\lambda$ is the square of an integer. Near these 'subresonant' straight lines in the shock diagram lie the 'fingers' within which the response does *not* tend to a single mode as $\nu \to \infty$. The form of the response within these fingers is still unclear except in certain special cases; all that is certain is that the amplitude is relatively large (for example, $\nu^{1/3}$ near the first finger $\lambda + \nu = 0$) and that shock solutions can be displayed explicitly in the case when $a(x)$ has just a few Fourier components (Keller 1977; Chester 1994). In fact, if we approximate $a'(x) = 2x$ by writing $a(x) = \sum_{n=1}^{N} [4(-1)^n/n^2] \cos nx$ for $N = 2, 4, 6$, an explicit calculation reveals figures 3(*a*)–3(*c*) respectively. Special cases in which $a(x)$ is harmonic have been considered in Chester (1994), in which figure 3(*a*, *b*) first appeared. The area between solid lines shows where shock solutions occur and the appearance of new fingers is associated with the sub-resonant lines.

(*b*) $\nu \sim O(\varepsilon^{-1/2})$. In this regime we are so far away from the one-dimensional scenario that it is easier not to think in terms of a generalized Chester's equation such as (1.17) but rather in terms of the commensurability of the spectrum. It appears from the discussions in Ockendon *et al.* (1993) that only when the nth eigenfrequency ω_n satisfies $|\omega_n - n| \ll \varepsilon^{1/2}$ is there a possibility of shocks and hence that there is likely to be a generic unimodal response unless these strong geometric variations are very special.

Although the parameter regime $h_0 \ll L$ precludes any obvious configurations in which the fundamental eigenfrequency is degenerate, the results that we will derive for 'non-thin' resonators near degeneracy in §2 will reveal an interesting similarity with the scenario illustrated in figure 3.

1.4. *The relationship between shallow water sloshing and acoustic resonance*

As explained in the penultimate paragraph of §1.1, we will only be able to see the relevance of our model (1.10), (1.14) to sloshing problems if we can incorporate the effects of dispersion into its predictions. Thus, before we go into a more detailed discussion of (1.15), (1.16), let us make some comments about its relationship with the shallow water problem; this will highlight the role of (1.15), (1.16) as the basic model for multi-dimensional non-dispersive resonance, to which terms can be appended later to account for dispersion. We can see this in the case of the rectangular tank modelled by (1.3), (1.5), (1.8) and (1.11) because when we use the shallow water scalings $h = \kappa\varepsilon^{1/4}$, $\lambda_0 = \lambda\varepsilon^{1/2}$, $\nu_0 = \nu\varepsilon^{1/2}$, $z = \varepsilon^{1/4}\bar{z}$, $\phi = \varepsilon^{-1/2}\bar{\phi}$ and $\eta = \varepsilon^{-1/4}\bar{\eta}$ (see Ockendon *et al.* 1986) in these equations, we find the shallow water model

$$\bar{\phi}_{\bar{z}\bar{z}} = -\varepsilon^{1/2}(\bar{\phi}_{xx} + \bar{\phi}_{yy}), \tag{1.18a}$$

$$\bar{\phi}_x = \varepsilon^{1/2} \sin t \quad \text{on} \quad x = -\varepsilon \cos t, \pi - \varepsilon \cos t, \tag{1.18b}$$

$$\bar{\phi}_y = 0 \quad \text{on} \quad y = 0, \tag{1.18c}$$

$$\bar{\phi}_y = \nu \frac{h_0}{L} \varepsilon^{1/2} \bar{\phi}_x a'(x) \quad \text{on} \quad y = \frac{h_0}{L}[1 + \nu \varepsilon^{1/2} a(x)], \tag{1.18d}$$

$$\bar{\phi}_{\bar{z}} = 0 \quad \text{on} \quad \bar{z} = -\kappa, \tag{1.18e}$$

where b has been replaced by h_0/L. The parameter κ will hereafter denote the measure of dispersion in the problem. The free surface conditions are

$$\bar{\phi}_{\bar{z}} = \varepsilon^{1/2} \bar{\eta}_t + \varepsilon \bar{\phi}_x \bar{\eta}_x + \varepsilon \bar{\phi}_y \bar{\eta}_y, \tag{1.18f}$$

$$\bar{\eta} + \kappa \left(1 + \varepsilon^{1/2} \left[\lambda - \tfrac{1}{3}\kappa^2\right]\right) \left(\bar{\phi}_t + \tfrac{1}{2}\left[\bar{\phi}_{\bar{z}}^2 + \varepsilon^{1/2}\left\{\bar{\phi}_x^2 + \bar{\phi}_y^2\right\}\right]\right) = 0, \tag{1.18g}$$

on $\bar{z} = \varepsilon^{1/2}\bar{\eta}$, correct to $O(\varepsilon)$. Then, expanding $\bar{\phi}$ and $\bar{\eta}$ as $\bar{\phi} = \phi_0 + \varepsilon^{1/2}\phi_1 + \varepsilon\phi_2 + \cdots$ and $\bar{\eta} = \eta_0 + \varepsilon^{1/2}\eta_1 + \varepsilon\eta_2 + \cdots$, we proceed to solve at each order to find $\phi_0 = A(x, y, t)$ and $\phi_1 = -\frac{1}{2}A_{tt}(\bar{z} + \kappa)^2 + B(x, y, t)$ where

$$A_{xx} + A_{yy} = A_{tt}, \tag{1.19a}$$

$$A_x = 0 \quad \text{on} \quad x = 0, \pi, \tag{1.19b}$$

$$A_y = 0 \quad \text{on} \quad y = 0, \frac{h_0}{L}, \tag{1.19c}$$

and

$$B_{xx} + B_{yy} - B_{tt} = -\tfrac{1}{3}\kappa^2 A_{tttt} + \left(\lambda - \tfrac{1}{3}\kappa^2\right) A_{tt} + 2A_x A_{xt} + 2A_y A_{yt} + A_t A_{tt}, \tag{1.20a}$$

$$B_x = \sin t \quad \text{on} \quad x = 0, \pi, \tag{1.20b}$$

$$B_y = 0 \quad \text{on} \quad y = 0, \tag{1.20c}$$

$$B_y = \nu \frac{h_0}{L}\left[A_x a'(x) - A_{yy} a(x)\right] \quad \text{on} \quad y = \frac{h_0}{L}, \tag{1.20d}$$

which clearly reduce to (1.15) and (1.16) when $\kappa = 0$ with $\gamma = 2$. Equally, following the ideas of Ockendon & Ockendon (1973), we can see that when $\kappa \to \infty$, the linear terms on the right-hand side of (1.20*a*) dominate so that $A_{tttt} + A_{tt} = 0$ which, together with (1.19), suggests that we can approximate A by $A = A_{1,0} \cos x \sin(t + \theta_1) + A_{0,1} \cos y \sin(t + \theta_2)$. A more detailed analysis is given in §2.4 to show that the amplitudes $A_{1,0}$ and $A_{0,1}$ satisfy (1.13) in the limit $h \to 0$, so that this deep water limit of the shallow water equations matches with the shallow water limit of our earlier deep water analysis. We will henceforth regard the effect of dispersion on the solution of (1.10), (1.14) as being to introduce fourth-order derivatives of the fundamental eigenmode into the formulation of the problem. In the case of purely two-dimensional motion (where the leading-order solution depends on just x and t) Ockendon *et al.* (1986) have shown that this has the effect of removing any possibility of shocks. The analysis becomes more and more complicated as κ decreases because the number of continuous periodic solutions appears to increase without bound; when $\kappa = 0$ there is a unique solution but it is discontinuous in a certain detuning range. A similar burgeoning of periodic solutions may be expected to occur in the three-dimensional case, but we will not investigate this here.

It is very difficult to model the effects of dissipation realistically in these resonance problems, but we instinctively expect viscous damping to 'round off' the large-amplitude branches in response diagrams such as figures 1 and 2. We will discuss this further in §3.

The picture that emerges from all the investigations described above is that acoustic and horizontally oscillated sloshing resonators exhibit Duffing-like responses unless the fundamental mode is degenerate or there is an infinite number of commensurate normal frequencies. This latter situation can only occur for special geometries, such as gas in a cylindrical organ pipe, and, when it does occur, there maybe a complicated response involving shock waves. A perturbation analysis for thin resonators reveals the ease with which this 'shock' response can be destroyed by geometric imperfections that remove the commensurability of the spectrum. However, there is as yet no analysis for resonators which are perturbations of configurations for which the spectrum is commensurate and exhibits degeneracy, say in the fundamental. Our model (1.10), (1.14) with $h_0/L = \pi$ applies to just such a situation and this is what we will study in the next two sections.†

2. Resonance with nearly commensurate and nearly degenerate spectra

In this section we will study (1.10), (1.14), (1.15) and (1.16) with $h_0/L = \pi$ in the simple but instructive case when $v_0 = O(\varepsilon^{1/2})$; we will leave all embellishments concerning other parameter regimes to §3.

The general periodic solution of (1.15), (1.16) is

$$A(x, y, t) = \sum_{p,q} \cos px \cos qy (a_{p,q} \cos \lambda_{p,q} t + b_{p,q} \sin \lambda_{p,q} t), \tag{2.1}$$

where $\lambda_{p,q}^2 = p^2 + q^2$ and p, q are integers such that the $\lambda_{p,q}$ are non-zero integers. It is convenient to write A as

$$A(x, y, t) = \sum_{i,j} A_{i,j}(x, y, t), \tag{2.2a}$$

where

$$A_{i,j} = f_{i,j}(t \pm l_{i,j} x \pm k_{i,j} y) \tag{2.2b}$$

are 2π-periodic plane waves in the $(\pm i, \pm j)$ directions, (i, j) denoting all the i, j such that $i^2 + j^2$ is the square of an integer and each pair (i, j) is coprime,

$$l_{i,j} = \frac{i}{\lambda_{i,j}}, \qquad k_{i,j} = \frac{j}{\lambda_{i,j}};$$

we have used the shorthand

$$\begin{aligned} f_{i,j}(t \pm l_{i,j} x \pm k_{i,j} y) = {} & f_{i,j}(t + l_{i,j} x + k_{i,j} y) + f_{i,j}(t + l_{i,j} x - k_{i,j} y) \\ & + f_{i,j}(t - l_{i,j} x + k_{i,j} y) + f_{i,j}(t - l_{i,j} x - k_{i,j} y). \end{aligned}$$

We will henceforth refer to the $f_{i,j}$ as the (i, j)-wavetrain. Thus we can, alternatively, write

$$A_{i,j}(x, y, t) = \sum_{s=1}^{\infty} \cos isx \cos jsy (a_{si,sj} \cos s\lambda_{i,j} t + b_{si,sj} \sin s\lambda_{i,j} t), \tag{2.3a}$$

where

$$f_{i,j}(\tau) = \frac{1}{d} \sum_{s=1}^{\infty} (a_{si,sj} \cos s\lambda_{i,j} \tau + b_{si,sj} \sin s\lambda_{i,j} \tau) \tag{2.3b}$$

† A further argument for studying (1.10), (1.14) is that it is unlikely that resonators with non-planar walls could ever sustain periodic responses including shocks, which would inevitably be curved, even if it had an infinite commensurate set of eigenvalues.

and $d = 2$ for $(i, j) = (1, 0)$ or $(0, 1)$ or $d = 4$ otherwise and the $f_{n,m}$ have been chosen to have zero mean without loss of generality. We will also find it convenient to have a Fourier series representation for $a(x)$, namely

$$a(x) = \sum_{n=0}^{\infty} \alpha_n \cos nx. \tag{2.4}$$

We now make some remarks about the application of the Fredholm Alternative to (1.16) using the form (2.2*b*) for $A(x, y, t)$. For a periodic solution of (1.16) to exist we need the forcing in this problem to be orthogonal to the doubly infinite set of eigensolutions to the homogeneous problem (1.15). We first multiply (1.16*a*) by the eigensolution $\cos npx \cos mpy G(t')$ where

$$G(t') = c_{np,mp} \cos(\lambda_{n,m} p t') + d_{np,mp} \sin(\lambda_{n,m} p t'),$$

and $c_{l,k}$ and $d_{l,k}$ are arbitrary constants. We then integrate over the whole domain and, using the boundary conditions (1.16*b–e*) and summing over p, find

$$\sum_{p=1}^{\infty} \int_0^{2\pi} \int_0^{\pi} \int_0^{\pi} F(x, y, t') \cos npx \cos mpy \, G(t') \mathrm{d}x \, \mathrm{d}y \, \mathrm{d}t'$$

$$= -\pi^2 \delta_{n1} \delta_{m0} d_{1,0} + \sum_{p=1}^{\infty} \int_0^{2\pi} \int_0^{\pi} B_y|_{y=\pi, t=t'} (-1)^{pm} \cos pnx \, G(t') \mathrm{d}x \, \mathrm{d}t' \tag{2.5}$$

for each (n, m), where $F(x, y, t)$ is the right-hand side of (1.16*a*). Before we can proceed any further we need the following result.

The expressions

$$\int_0^{2\pi} \int_0^{\pi} \int_0^{\pi} A_{n_1,m_1} A_{n_2,m_2} \cos qn_3 x \cos qm_3 y \left\{ \begin{array}{c} \cos q\lambda_{n_3,m_3} t' \\ \sin q\lambda_{n_3,m_3} t' \end{array} \right\} \mathrm{d}x \, \mathrm{d}y \, \mathrm{d}t', \tag{2.6}$$

where $q = 1, 2, \ldots$ *and the pairs* (n_i, m_i) *are coprime are non-zero if and only if* $n_1 = n_2 = n_3$ *and* $m_1 = m_2 = m_3$. The proof is a straightforward case-by-case enumeration (see Waterhouse 1995) so we do not give it here.

Noting that most of the terms in $F(x, y, t)$ are quadratic in A, this result states that the only terms in $F(x, y, t)$ for the (n, m) set of orthogonality relations (2.5) that do not integrate to zero in the left-hand side are those containing only products of $A_{n,m}$ (or $f_{n,m}$). Hence we can replace F in (2.5) by $F_{n,m}$ where

$$F_{n,m}(x, y, t) = \lambda (A_{n,m})_{tt} + 2(A_{n,m})_x (A_{n,m})_{xt} + 2(A_{n,m})_y (A_{n,m})_{yt} + (\gamma - 1)(A_{n,m})_t (A_{n,m})_{tt}.$$

The left-hand side of (2.5) can now be integrated explicitly, and putting $c_{np,mp} = \cos \lambda_{n,m} pt$, $d_{np,mp} = \sin \lambda_{n,m} pt$ and, using the method of §3 of Ockendon *et al.* (1993) to evaluate the sum in the left-hand side of (2.5), we finally find that the $f_{n,m}$ satisfy

$$\mathscr{C} f_{n,m} + \frac{1}{\pi} \sin t \, \delta_{n1} \delta_{m0} = -\frac{2m^2 \alpha_0 \nu}{\lambda_{n,m}^2} f''_{n,m} + \frac{\nu}{\pi^2} \sum_{p=1}^{\infty} \int_0^{2\pi} \int_0^{\pi} R(x, t') (-1)^{pm} \cos pnx \cos p\lambda_{n,m} (t' - t) \mathrm{d}x \, \mathrm{d}t'; \tag{2.7}$$

here $\mathscr{C} f_{n,m}$ is shorthand for

$$\mathscr{C} f_{n,m} = \lambda f''_{n,m}(t) + (\gamma + 1) f'_{n,m}(t) f''_{n,m}(t), \tag{2.8}$$

the right-hand side is linear in $f_{n,m}$ with

$$R(x,t) = a'(x)A_x(x,\pi,t) - (a(x)-\alpha_0)A_{yy}(x,\pi,t), \tag{2.9}$$

and α_0 is the mean value of $a(x)$.

The set of equations (2.7) will form the basis for all our subsequent discussions. Their most interesting feature is the complication caused by the term $R(x,t)$ which involves, in general, a coupling between *all* the $A_{i,j}$ and the Fourier coefficients of $a(x)$ and hence the right-hand side of (2.7) contains all the $f_{i,j}$. For example, we find, in the case $(n,m) = (1,0)$, that (2.7) gives

$$\begin{aligned}\mathscr{C}f_{1,0} + \frac{1}{\pi}\sin t = &-\frac{\nu}{2\pi}\int_0^{\pi}[a'(\pi-t') - a'(t')][f'_{1,0}(t+2t') + \cdots]\mathrm{d}t' \\ &-\frac{\nu}{\pi}\int_0^{\pi} a'(\pi-t')[f'_{0,1}(t+t') - f'_{0,1}(t-t') + \cdots]\mathrm{d}t',\end{aligned} \tag{2.10}$$

where only the first two wavetrains have been included. However, we will later exploit the fact that the form of this right-hand side simplifies in three special cases, two of which have been already mentioned in §1:

(i) when $a'(x)$ is linear in x, i.e. the back wall is parabolic, the equations reduce to a set of ordinary differential equations where, for example, (2.10) reduces to

$$\mathscr{C}f_{1,0} = -\frac{1}{\pi}\sin t + \nu\left(f_{1,0} + 4f_{0,1} + \cdots\right);$$

(ii) when $a(x)$ has a finite number of Fourier components, a reduced, but still infinite number of $f_{i,j}$ occur on the right-hand side of (2.7);

(iii) when $a'(x) = a'(\pi - x)$, i.e. the back is anti-symmetric, we see, for, example, that (2.10) simplifies and, in general, the right-hand side of (2.7) will again contain a reduced number of $f_{i,j}$.

Before considering (2.7) in detail, there are two general points that need to be enunciated that we will need in the later discussions.

The first concerns the uniqueness of physically acceptable solutions of nonlinear wave equations in the presence of weak shocks. For shocks of arbitrary strength, uniqueness can be demonstrated on the basis of entropy, stability or viscosity arguments, the choice being usually dictated by technical considerations. For the weak shocks considered in this paper, a trivial one-dimensional stability argument shows that perturbations to a constant-velocity shock can only die away from the shock if it is compressive. Hence this criterion will be used to select weak shocks throughout the rest of this manuscript.

Our second general point concerns the two-dimensional intersection of two straight shocks of different families (as discussed in Liepmann & Roshko 1957). When such shocks have arbitrary strength, several different downstream configurations are possible but, in the weak shock limit, the vortex sheet or slipstream shed from the intersection point is of second order in strength compared to the shock strength. Hence, when we encounter such intersections later in this section, we will assume the shocks pass through each other without change of strength and without creating any new discontinuity.

We now return to (2.7); there are several limiting cases that we will need as reference points before we can make any general statement about the response. One immediate observation is that as α_0 gets large with $\nu \neq 0$, we move away from the nearly square resonator and (2.7) implies that $f_{n,m} \sim O(1/\alpha_0)$ for $(n,m) \neq (1,0)$ and $f_{1,0}$ satisfies (1.2) to leading-order.

2.1. *The limit* $\nu \to 0$

When $\nu = 0$, (2.7) collapses into Chester's equation (1.2) for $f_{1,0}$. This equation must be solved under the conditions that $f_{1,0}$ is periodic and, since φ_0 is the velocity potential, $f_{1,0}$ is continuous, together with the restriction that any discontinuity in $f'_{1,0}$ corresponds to a compressive shock. The unique solution for $|\lambda| < \lambda^* = 4[(\gamma+1)/\pi^3]^{1/2}$ is given by

$$f'_{1,0} + \frac{\lambda}{\gamma+1} = \left(\frac{4}{\pi(\gamma+1)}\right)^{1/2} \begin{cases} \cos\tfrac{1}{2}t, & -\pi < t < t_0^*, \\ -\cos\tfrac{1}{2}t, & t_0^* < t < \pi, \end{cases} \tag{2.11a}$$

where t_0^* is given in terms of λ by

$$\lambda = 4\left(\frac{\gamma+1}{\pi^3}\right)^{1/2} \sin\tfrac{1}{2}t_0^*. \tag{2.11b}$$

When we now consider ν to be small and positive, we see from (2.7) that, for $\lambda = O(1)$, $f_{1,0} \sim O(1)$ but all the other $f_{n,m}$ are of $O(\nu)$. Hence we write

$$f_{n,m} = \delta_{n1}\delta_{m0} f_{n,m}^{(0)} + \nu f_{n,m}^{(1)} + \cdots,$$

to give that $f_{1,0}^{(0)}$ satisfies (2.11) and

$$\lambda f_{n,m}^{(1)''} + (\gamma+1)\left(f_{n,m}^{(0)'} f_{n,m}^{(1)''} + f_{n,m}^{(1)'} f_{n,m}^{(0)''}\right)\delta_{n1}\delta_{m0}$$
$$= \frac{1}{\pi^2}\sum_{p=1}^{\infty}\int_0^{2\pi}\int_0^{\pi} R^{(0)}(x,t')(-1)^{pm}\cos pnx \cos p\lambda_{n,m}(t'-t)\,\mathrm{d}x\,\mathrm{d}t', \tag{2.12}$$

where $R^{(0)}(x,t) = [f_{1,0}^{(0)'}(t+x) - f_{1,0}^{(0)'}(t-x)]a'(x)$. Note that the first term on the right-hand side of (2.7) has no effect at this order, so the solutions considered throughout this subsection are independent of the choice of α_0. The effects of the geometry can now be considered in terms of

(i) the modulation of the one-dimensional solution described by the linear equation (2.12) with $(n,m) = (1,0)$ and

(ii) the excitation of cross-wavetrains which are described by the linear equations (2.12) with $(n,m) \neq (1,0)$.

To discuss the modulation of the one-dimensional solution, we write the shock location as

$$t^* = t_0^* + \nu t_1^* + \cdots,$$

and solve a perturbed free boundary problem for $f'_{1,0}$. Thus the continuity condition $[f_{1,0}] = 0$ implies

$$[f_{1,0}^{(1)}] = -t_1^*[f_{1,0}^{(0)'}], \tag{2.13}$$

where square brackets denote jumps from $t_0^* - 0$ to $t_0^* + 0$. We can minimize the algebraic complexity by choosing the special case $a'(x) = 2x$, in which case we can integrate (2.12) for $(n,m) = (1,0)$ to give

$$2\left(\frac{\gamma+1}{\pi}\right)^{1/2}(\cos\tfrac{1}{2}t)\, f_{1,0}^{(1)'} = \frac{\lambda}{2(\gamma+1)}(\pi^2 - t^2) + \frac{4}{[\pi(\gamma+1)]^{1/2}}\left(d_1(t+\pi) - 2\cos\tfrac{1}{2}t\right), \quad -\pi < t < t_0^*,$$

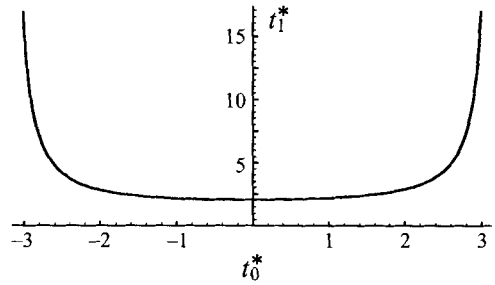

FIGURE 4. Plot of t_1^* against t_0^* where the shock is located at $t^* = t_0^* + \nu t_1^*$.

and

$$-2\left(\frac{\gamma+1}{\pi}\right)^{1/2}(\cos\tfrac{1}{2}t)\,f_{1,0}^{(1)'} = \frac{\lambda}{2(\gamma+1)}(\pi^2 - t^2)$$
$$+\frac{4}{[\pi(\gamma+1)]^{1/2}}\left(d_1\pi + d_2 t - 4\cos\tfrac{1}{2}t_0^* - 2t_0^*\sin\tfrac{1}{2}t_0^* + 2\cos\tfrac{1}{2}t\right), \quad t_0^* < t < \pi.$$

Hence $f_{1,0}^{(1)}$ is periodic if

$$d_1 = \frac{1}{\pi}\left[2\cos\tfrac{1}{2}t_0^* + (t_0^* - \pi)\sin\tfrac{1}{2}t_0^*\right],$$
$$d_2 = \frac{1}{\pi}\left[2\cos\tfrac{1}{2}t_0^* + (t_0^* + \pi)\sin\tfrac{1}{2}t_0^*\right],$$

and we can use (2.13) to find t_1^*. The result is plotted in figure 4 for $\gamma = 1.4$, in which the singularity as $|\lambda| \to \lambda^*$ indicates that an inner expansion is needed to describe the way in which the shock regime in the shock diagram shifts slightly as ν increases from zero (see figure 3). It can also be shown that the strength of the perturbed discontinuity in $f_{1,0}^{(0)'} + \nu f_{1,0}^{(1)'}$ decreases for $\lambda > 0$ and increases for $\lambda < 0$ in accordance with this shift in the shock regime and this behaviour applies qualitatively to more general $a(x)$ (Waterhouse 1995).

When we come to illustrate the 'cross-wavetrains' $f_{n,m}$ for $(n,m) \neq (1,0)$, it is convenient to revert to the representation (2.3) and write

$$f_{1,0}^{(0)} = \frac{1}{2}\sum_{n=1}^{\infty}(a_{n,0}^{(0)}\cos nt + b_{n,0}^{(0)}\sin nt),$$

and also to write $a(x)$ in terms of its Fourier series (2.4). To avoid undue complications we only show the results corresponding to the second term in the Fourier series for $a(x)$ by taking $a(x) = \cos x$. The other terms can be treated similarly. In this case, with $\lambda \sim O(1)$, (2.12) gives

$$f_{0,1}^{(1)} = \frac{1}{2\lambda}(a_{1,0}^{(0)}\cos t + b_{1,0}^{(0)}\sin t), \quad f_{4,3}^{(1)} = \frac{1}{20\lambda}(a_{5,0}^{(0)}\cos 5t + b_{5,0}^{(0)}\sin 5t), \tag{2.14}$$

and so on where $f_{n,m}^{(1)} = 0$ unless $\lambda_{n,m} - n = 1$. We soon see that as $n^2 + m^2 \to \infty$, $f_{n,m}^{(1)} \sim (n^2 + m^2)^{-5/2}$, but, more importantly, the lowest-order cross-wavetrain is a purely harmonic response with an amplitude that decreases for higher wavenumbers, even though we are in a situation with a degenerate spectrum.

However, there is one interesting regime in which the degeneracy has a dramatic effect, as can be discerned from (2.14). This is when λ is so small that a rescaling

of (2.7) is necessary in order to keep the nonlinearity in balance with the detuning. In fact we can see the existence of a fine detuning band near $\lambda = 0$ on physical grounds by noting that the primary forcing of $O(\varepsilon)$ produces a primary response of $O(\varepsilon^{1/2})$, and hence a cross-wavetrain forcing (due to the interaction of the $O(\nu\varepsilon^{1/2})$ geometry variation with this response) of $O(\nu\varepsilon)$; then, because of the degeneracy of the fundamental, the cross wavetrain response is of $O(\nu\varepsilon^{1/2})$. Indeed, inspection of (2.7) shows that we need to write

$$\lambda = \nu^{1/2}\tilde{\lambda} \quad , \quad f_{n,m} = \nu^{1/2} g^{(1)}_{n,m} + \cdots,$$

in order to retain the nonlinear terms in the limit $\nu \to 0$. This leads to

$$\tilde{\lambda} g^{(1)''}_{n,m} + (\gamma+1) g^{(1)'}_{n,m} g^{(1)''}_{n,m} = \frac{1}{\pi^2} \sum_{p=1}^{\infty} \int_0^{2\pi} \int_0^{\pi} R^{(0)}(x,t')(-1)^{pm} \cos pnx \cos p\lambda_{n,m}(t'-t)\,dx\,dt', \tag{2.15}$$

for all $(n,m) \neq (1,0)$, with $f_{1,0}$ given by (2.11*a*) and, from (2.11*b*),

$$t_0^* = \frac{1}{2}\left(\frac{\pi^3}{\gamma+1}\right)^{1/2} \nu^{1/2}\tilde{\lambda}.$$

We now have the possibility of a much more interesting cross-wavetrain response. Equations (2.11*a*) and (2.15) give

$$\left(g^{(1)'}_{0,1} + \frac{\tilde{\lambda}}{\gamma+1}\right)^2 = \frac{32}{3}[(\gamma+1)\pi]^{-3/2}[c_1 - \sin t], \tag{2.16a}$$

$$\left(g^{(1)'}_{4,3} + \frac{\tilde{\lambda}}{\gamma+1}\right)^2 = \frac{16}{99}[(\gamma+1)\pi]^{-3/2}[c_2 - \sin 5t], \tag{2.16b}$$

and so on for higher-order wavetrains, where c_1, c_2 are constants. Consideration of these expressions shows that discontinuous solutions for $g^{(1)}_{0,1}$ occur for $|\tilde{\lambda}| < 1.3(\gamma+1)^{1/4}$ and for $g^{(1)}_{4,3}$ when $|\tilde{\lambda}| < 0.2(\gamma+1)^{1/4}$. To highlight this we consider the case $\tilde{\lambda} = 0$, so

$$g^{(1)'}_{0,1} = \left(\frac{32}{3}\right)^{1/2}[(\gamma+1)\pi]^{-3/4} \begin{cases} (1-\sin t)^{1/2} & -\frac{3}{2}\pi < t < -\frac{1}{2}\pi, \\ -(1-\sin t)^{1/2} & -\frac{1}{2}\pi < t < \frac{1}{2}\pi, \end{cases}$$

$$g^{(1)'}_{4,3} = \left(\frac{16}{99}\right)^{1/2}[(\gamma+1)\pi]^{-3/4} \begin{cases} (1-\sin 5t)^{1/2} & -\frac{11}{10}\pi < t < -\frac{1}{10}\pi, \\ -(1-\sin 5t)^{1/2} & -\frac{1}{10}\pi < t < \frac{9}{10}\pi, \end{cases}$$

and so on, where the interaction of the shocks in these solutions with that of the primary wavetrain has been assumed to create no new discontinuities as explained on page 328. We illustrate this case, plotting A_t (which is proportional to the pressure) at $t = -\pi/4$ for $\gamma = 1.4$ in figure 5(*a*) for $\nu = 0$ and figure 5(*b*) for $\nu = 0.2$ (with just the first three wavetrains). The $f_{4,3}$-wavetrain can just be seen and the introduction of further wavetrains has a negligible effect.

Consideration of other forms of $a(x)$ that contain just a finite number of Fourier components confirms that in all cases the primary wavetrains ($f_{1,0}$ and $f_{0,1}$) are much larger than the higher-order wavetrains.

2.2. *The limits* $\lambda, \nu \to \infty$

In this parameter regime, we can carry out an analysis in the same spirit as that on page 324 to see that each $f_{n,m}$ is of $O(1/\nu)$ except in certain thin regions when there

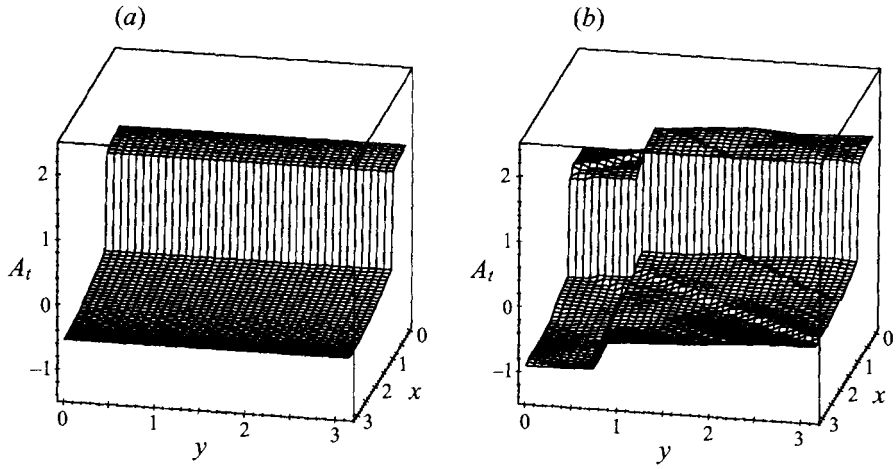

FIGURE 5. Plot of A_t for $\lambda = 0$, $a(x) = \cos x$ and (*a*) $\nu = 0$, (*b*) $\nu = 0.2$.

is a 'subresonance'. Hence we propose that as $\lambda, \nu \to \infty$ with $\lambda = O(\nu)$

$$f_{n,m} = \frac{1}{\nu} f^{(0)}_{n,m} + \frac{1}{\nu^3} f^{(1)}_{n,m} + \frac{1}{\nu^5} f^{(2)}_{n,m} + \cdots.$$

Now it is straightforward to see that if, for example, $a(x) = \alpha_0 + \alpha_1 \cos x$,

$$f_{1,0} = \frac{\lambda + 2\alpha_0 \nu}{\pi(\lambda^2 + 2\alpha_0 \lambda \nu - \alpha_1^2 \nu^2)} \sin t - \frac{(\gamma+1)(\lambda + 2\alpha_0 \nu)^2}{8\pi^2 \lambda (\lambda^2 + 2\alpha_0 \lambda \nu - \alpha_1^2 \nu^2)^2} \sin 2t + \cdots, \tag{2.17a}$$

$$f_{0,1} = \frac{\alpha_1 \nu}{\pi(\lambda^2 + 2\alpha_0 \lambda \nu - \alpha_1^2 \nu^2)} \sin t - \frac{(\gamma+1)\alpha_1^2 \nu^2}{8\pi^2 (\lambda + 2\alpha_0 \nu)(\lambda^2 + 2\alpha_0 \lambda \nu - \alpha_1^2 \nu^2)^2} \sin 2t + \cdots, \tag{2.17b}$$

$$f_{n,m} = O\left(\nu^{1-2(n^2+m^2)^{1/2}}\right). \tag{2.17c}$$

Hence the first mode in the primary wavetrains blows up close to the perturbed eigenvalues, or 'spectral lines', given in the shock diagram by

$$\lambda = \left[-\alpha_0 \pm \left(\alpha_0^2 + \alpha_1^2\right)^{1/2}\right] \nu. \tag{2.18}$$

A rescaling similar to that employed in Ockendon *et al.* (1993) shows that as we approach the detuning range $\lambda + \bar{\alpha}\nu = \hat{\lambda} \nu^{-1/3}$, where $\bar{\alpha} = \alpha_0 - (\alpha_0^2 + \alpha_1^2)^{1/2}$, we find the Duffing-like response

$$f_{1,0} = A \nu^{1/3} \sin t + O(\nu^{-1/3}),$$

$$f_{0,1} = -\frac{\bar{\alpha}}{\alpha_1} A \nu^{1/3} \sin t + O(\nu^{-1/3}),$$

where

$$\hat{\lambda} A \left(1 + \frac{\bar{\alpha}^2}{\alpha_1^2}\right) - \frac{(\gamma+1)^2}{8\bar{\alpha}} A^3 \left(1 + \frac{\bar{\alpha}^4}{\alpha_1^4}\right) = \frac{1}{\pi}. \tag{2.19}$$

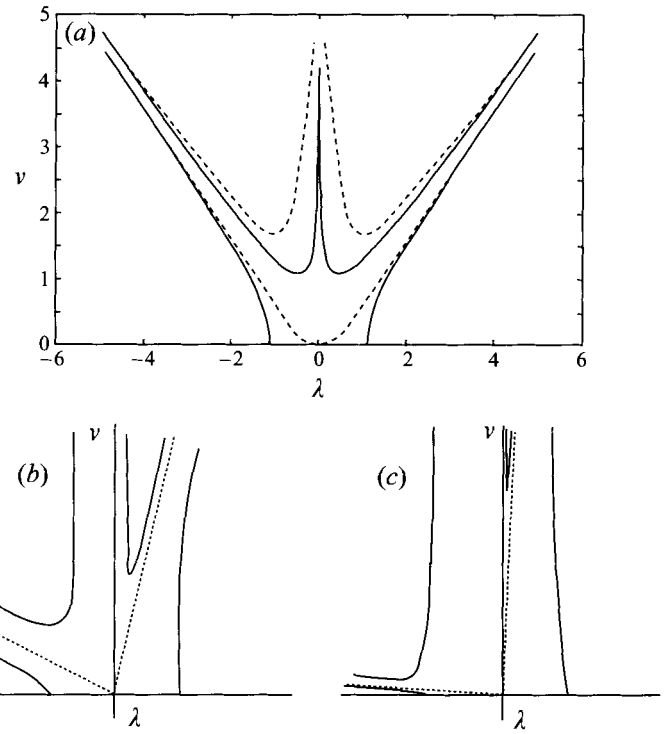

FIGURE 6. Shock diagrams showing, for $a(x) = \alpha_0 + \cos x$ and $\gamma = 1.4$, the interface between shock and continuous solutions in the cases (*a*) $\alpha_0 = 0$, (*b*) $\alpha_0 = 1$ and (*c*) $\alpha_0 = 10$. In (*a*), there are shocks in the longitudinal direction between the solid lines and shocks in the transverse direction between the dashed lines. In (*b*) and (*c*), shocks are found in between the solid lines and the dotted lines represent the spectral lines (2.18).

As $\hat{\lambda} \to \infty$, the larger-amplitude response grows from $O(\nu^{1/3})$ to $O(\nu)$ and the other modes re-enter the solution and shocks are possible. The situation is reminiscent of the large imperfection limit of the thin resonators discussed on page 324 except that, even though there is only one harmonic in $a(x)$, there are two fingers in whose neighbourhood (2.19) holds. This is shown in the large-ν portion of the shock diagram figure 6(*a*) which illustrates the case $\alpha_0 = 0$, $\alpha_1 = 1$ and is drawn accurately; the solution within these fingers contains shocks of comparable amplitude travelling in both the x- and y-directions. Figures 6(*b*) and 6(*c*) show the cases $\alpha_0 = 1$, $\alpha_1 = 1$ and $\alpha_0 = 10$, $\alpha_1 = 1$ schematically to indicate how the one-dimensional Chester response is retrieved as $\alpha_0 \to \infty$. When $a(x)$ contains higher Fourier coefficients there are more fingers in the shock diagram; the details can be found in Waterhouse (1995), where it is shown that the first three modes in the primary wavetrains dominate the leading-order terms in (2.17) for all λ and ν.

2.3. *An iterative procedure for* $\nu \sim O(1)$

Let us now return to (2.7) for $\nu \sim O(1)$ so that no obvious analytical simplification is possible. We recall that the limiting solutions found in §2.1 and §2.2 have a recurring theme in that, in all cases, modes associated with the two primary wavetrains, $f_{1,0}$ and $f_{0,1}$, have dominated the solution. Thus we propose the following iteration scheme:

we write (2.7) as

$$\mathscr{C}f_{n,m}^{(i+1)} + \frac{1}{\pi}\sin t\delta_{n1}\delta_{m0} = -\frac{2m^2\alpha_0 v}{\lambda_{n,m}^2} f_{n,m}^{(i)''} + \frac{v}{\pi^2}\sum_{p=1}^{\infty}\int_0^{2\pi}\int_0^{\pi} R^{(i)}(x,t')(-1)^{pm}\cos pnx\cos p\lambda_{n,m}(t'-t)\mathrm{d}x\,\mathrm{d}t', \quad (2.20)$$

where $f_{n,m}^{(i+1)}$ is the $(i+1)$th approximation to $f_{n,m}$ and $R^{(i)}$ is the expression found for R by using the approximations $f_{n,m}^{(i)}$ for the $f_{n,m}$. We take as our initial approximation

$$A(x,y,t) = f_{1,0}^{(0)}(t \pm x) + f_{0,1}^{(0)}(t \pm y),$$

so our starting values for the $f_{n,m}$ are

$$f_{n,m}^{(0)} = 0, \quad (n,m) \neq (1,0) \quad \text{or} \quad (0,1), \quad (2.21)$$

where $f_{1,0}^{(0)}$ and $f_{0,1}^{(0)}$ satisfy (2.7) with $f_{n,m}$ ($(n,m) \neq (1,0)$ or $(0,1)$) formally set to zero, namely

$$\mathscr{C}f_{1,0}^{(0)} = -\frac{1}{\pi}\sin t + \frac{v}{2\pi}\int_0^{\pi}[a'(t') - a'(\pi - t')]f_{1,0}^{(0)'}(t+2t')\mathrm{d}t' + \frac{v}{\pi}\int_0^{\pi} a'(\pi - t')[f_{0,1}^{(0)'}(t-t') - f_{0,1}^{(0)'}(t+t')]\mathrm{d}t', \quad (2.22a)$$

$$\mathscr{C}f_{0,1}^{(0)} = \frac{v}{\pi}\int_0^{\pi} a'(\pi - t')[f_{1,0}^{(0)'}(t-t') - f_{1,0}^{(0)'}(t+t')]\mathrm{d}t' - 2v\alpha_0 f_{0,1}^{(0)''}. \quad (2.22b)$$

We may estimate the rate of convergence by noting that $a_{k,0}$ and $a_{0,k}$ are $O(1/k^3)$ for continuous solutions and $O(1/k^2)$ for shock solutions as follows. Consider the contribution from $f_{1,0}^{(0)}$ or $f_{0,1}^{(0)}$ to the right-hand side of (2.20) for $i = 0$. This feedback term in the equation for $f_{n,m}^{(1)}$ contains a term involving $a_{(n^2+m^2)^{1/2},0}$ from the $f_{1,0}^{(0)}$-wavetrain. Hence, bearing in mind the definitions (2.3b) for $f_{n,m}$ and the size of the $a_{k,0}$, it is consistent that $f_{n,m}^{(1)} \sim O(\lambda_{n,m}^{-5})$ for continuous solutions and $f_{n,m}^{(1)} \sim O(\lambda_{n,m}^{-4})$ for shock solutions. This argument indicates that the higher-order wavetrains have an amplitude that is smaller numerically than the primary wavetrains by a factor of at least $(n^2+m^2)^{-2}$.

We now demonstrate the effectiveness of this iterative procedure by applying it to the case $a(x) = \alpha_0 + \alpha_1\cos x$, where we have already found that the cross-wavetrains are described by (2.12) and (2.15) when $v \to 0$. We consider the first step in the iteration where (2.22) gives

$$\mathscr{C}f_{1,0}^{(0)} = -\sin t\left[\frac{1}{\pi} + \tfrac{1}{2}\alpha_1 v b_{0,1}^{(0)}\right] - \tfrac{1}{2}\alpha_1 v a_{0,1}^{(0)}\cos t,$$

$$\mathscr{C}f_{0,1}^{(0)} = -\tfrac{1}{2}\alpha_1 v\left[b_{1,0}^{(0)}\sin t + a_{1,0}^{(0)}\cos t\right] - 2v\alpha_0 f_{0,1}^{(0)''}.$$

These equations can be solved using an approach similar to that of Chester (1994) (see Waterhouse 1995) and for v small, the range for shocks emerging in the $f_{0,1}$-wavetrain agrees with the predictions of §2.1. The algebra is very complicated and we only carry out a full analysis for the special case of 'extreme degeneracy' when

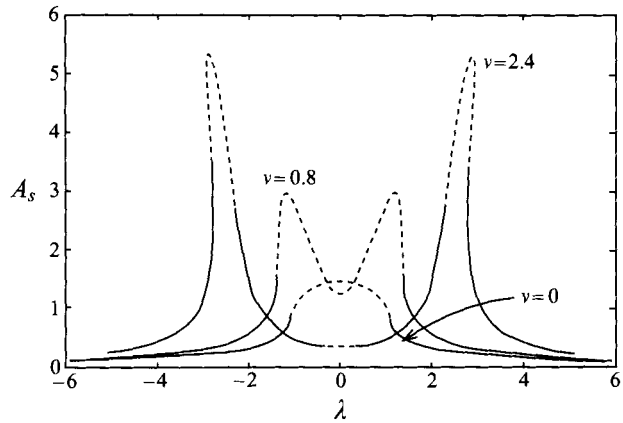

FIGURE 7. Response diagram showing, for $a(x) = \cos x$ and $\gamma = 1.4$, the response where there the dashed part of the curve indicates a shock in either direction.

$\alpha_0 = 0$ and $\alpha_1 = 1$ to find figure 6(*a*) which shows the different parameter regimes in the shock diagram with the now familiar shock response in fingers near the perturbed eigenvalues $\lambda = \pm\nu$. In between the solid lines (in the same sense as in figure 3) we find a shock in the $f_{1,0}$-wavetrain and in between the dashed lines a shock in the $f_{0,1}$-wavetrain. As in the case when ν is small, we have neglected any discontinuities that might be generated by the shock intersection. As pointed out earlier this shock diagram is different from its one-dimensional equivalent in that there are now two fingers associated with the introduction of one harmonic in $a(x)$. This is due to the coupling between the two wavetrains, while the symmetry about the line $\lambda = 0$ in this case is just a consequence of taking $a(x) = \cos x$. A schematic of the shock diagram we expect for $\alpha_0 = 1, 10$ and $\alpha_1 = 1$ is shown in figures 6(*b*) and 6(*c*) to illustrate, for $\nu \sim O(1)$, how the one-dimensional Chester response emerges as $\alpha_0 \to \infty$. In these diagrams, the dotted lines are the spectral lines (2.18) and we recall, from (2.7), that, as $\alpha_0 \to \infty$, $f_{0,1} \sim O(1/\alpha_0)$ and the longitudinal wavetrain dominates for all λ, ν as α_0 grows large.

To illustrate the response we recall that A_t is proportional to the pressure in the gas and that $A_t(0,0,t) = 2(f_{1,0}^{(0)'} + f_{0,1}^{(0)'})$ so we take as a typical amplitude

$$A_s = \left\{\left(\max f_{1,0}^{(0)'} - \min f_{1,0}^{(0)'}\right) + \left(\max f_{0,1}^{(0)'} - \min f_{0,1}^{(0)'}\right)\right\},$$

and this is plotted in figure 7 against the detuning for various values of ν. This choice of A_s also allows us to compare figure 7 with figure 2. Although there is no dispersion in the former, the resonant peaks are at similar locations but are distorted by dispersion in figure 2. The two Duffing-type branches correspond to the growth of the $\sin t$ term in the expansions for $f_{1,0}$ and $f_{0,1}$ and the right-hand branch matches very well with the formula (2.19) even for values of ν as small as 2. In figure 8 we plot A_t at $t = -\pi/4$, for $\lambda = 0$, $\nu = 1$ which can be compared to figure 5(*b*) and we see the growth of the $f_{0,1}$-wavetrain and a change in its phase.

Proceeding to the next stage of our iteration we have, from (2.20), $f_{1,0}^{(1)} = f_{1,0}^{(0)}$, $f_{0,1}^{(1)} = f_{0,1}^{(0)}$, $f_{3,4}^{(1)} = 0$ and

$$\mathscr{C} f_{4,3}^{(1)} = -\tfrac{5}{4}\nu\left[a_{5,0}^{(0)}\cos 5t + b_{5,0}^{(0)}\sin 5t\right],$$

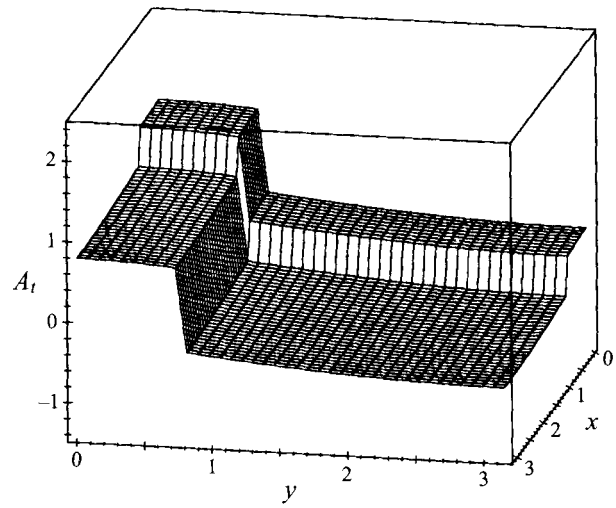

FIGURE 8. Plot of A_t for $\lambda = 0$, $\nu = 1$, $t = -\pi/4$ and $\gamma = 1.4$.

and so on for the other $f^{(1)}_{n,m}$. It is possible to solve these equations and then proceed to the next stage of the iteration. Calculations of the wavetrains to this second order of approximation have been found to affect the original approximations only by a few percent.

2.4. *Dispersive effects*

As mentioned in the introduction, we can only see the relevance of the above analysis (based as it is on the acoustic model (1.15), (1.16)) to sloshing resonance if we consider the effects of weak dispersion and thereby attempt to retrieve (1.12), (1.13). To do this we note that if we had considered the shallow water problem (1.19) and (1.20) instead of the acoustic problem we would have found that (2.7) is modified by the strength of the forcing becoming $2/\pi$ and that $\mathscr{C}f_{n,m}$ is now

$$\mathscr{C}f_{n,m} = -\tfrac{1}{3}\kappa^2 f^{(\mathrm{iv})}_{n,m} + \left(\lambda - \tfrac{1}{3}\kappa^2\right) f''_{n,m} + 3f'_{n,m}f''_{n,m}. \tag{2.23}$$

We can now retrieve the result in §1.3 on the deep water limit of this shallow water solution by letting $\kappa \to \infty$ in (2.7) with the modifications just discussed. Firstly, we note that the shallow water limit of (1.12) and (1.13) as $h \to 0$ gives

$$\phi \sim \varepsilon^{1/3}[A\cos x \sin(t+\theta_1) + B\cos y \sin(t+\theta_2)], \tag{2.24}$$

with $\sin\theta_1 = \sin\theta_2 = 0$ and

$$\frac{4}{\pi} = \left(\lambda_d A - \frac{9}{32h^2}A^3 - \tfrac{1}{4}AB^2 + \nu_d\alpha_2 A\right)\cos\theta_1 - \nu_d\alpha_1 B\cos\theta_2,$$

$$0 = \left(\lambda_d B - \frac{9}{32h^2}B^3 - \tfrac{1}{4}A^2B + 2\nu_d\alpha_0 B\right)\cos\theta_2 - \nu_d\alpha_1 A\cos\theta_1,$$

where α_0, α_1 and α_2 are the Fourier coefficients defined in (2.4). Using the shallow water scalings of §1.4 and scaling A and B as

$$A = \kappa^{2/3}\varepsilon^{1/6}A^*, \quad B = \kappa^{2/3}\varepsilon^{1/6}B^*,$$

yields

$$\frac{4}{\pi} = \left(\lambda\kappa^{2/3}A^* - \tfrac{9}{32}A^{*3} + \nu\kappa^{2/3}\alpha_2 A^*\right)\cos\theta_1 - \nu\kappa^{2/3}\alpha_1 B^*\cos\theta_2 \qquad (2.25a)$$

$$0 = \left(\lambda\kappa^{2/3}B^* - \tfrac{9}{32}B^{*3} + 2\nu\kappa^{2/3}\alpha_0 B^*\right)\cos\theta_2 - \nu\kappa^{2/3}\alpha_1 A^*\cos\theta_1 \qquad (2.25b)$$

plus $O(\varepsilon^{1/2}\kappa^2)$ terms, where we have written $\lambda_d = \lambda\varepsilon^{-1/6}$, $\nu_d = \nu\varepsilon^{-1/6}$, relating the deep water scalings to the shallow water scalings. To consider the deep water limit of (2.7) with (2.23) as $\kappa \to \infty$, we recall that the shallow water depth is $O(\varepsilon^{1/4})$ and the detuning range is $\lambda_0 \sim O(\varepsilon^{1/2})$. To match to the deep water scalings we require $\kappa \sim O(\varepsilon^{-1/4})$ and $\lambda \sim O(\varepsilon^{1/6})$ (so that we are in the detuning range $\lambda_0 \sim O(\varepsilon^{2/3})$) and hence we take the limit as $\kappa \to \infty$ with $\lambda\kappa^{2/3} \sim O(1)$. Similarly we require $\nu\kappa^{2/3} \sim O(1)$ for the correct scaling of ν_0 and we expand the $f_{n,m}$ as

$$f_{n,m} = \kappa^{2/3}f^{(0)}_{n,m} + \kappa^{-2/3}f^{(1)}_{n,m} + \kappa^{-2}f^{(2)}_{n,m} + \cdots \quad \forall(n,m).$$

Solving the $O(\kappa^{8/3})$ problem gives

$$f^{(0)}_{n,m} = A_{n,m}\sin(t + \theta_{n,m}) \quad \forall(n,m). \qquad (2.26)$$

Solving for $f^{(1)}_{n,m}$ and then applying the Fredholm Alternative to the $f^{(2)}_{n,m}$ problem gives $\sin\theta_{n,m} = 0$ and

$$\left.\begin{aligned} 2/\pi &= \left(\lambda\kappa^{2/3} - \tfrac{9}{8}A^2_{1,0} + \alpha_2\nu\kappa^{2/3}\right)A_{1,0}\cos\theta_{1,0} - \alpha_1\nu\kappa^{2/3}A_{0,1}\cos\theta_{0,1}, \\ 0 &= \left(\lambda\kappa^{2/3} - \tfrac{9}{8}A^2_{0,1} + 2\alpha_0\nu\kappa^{2/3}\right)A_{0,1}\cos\theta_{0,1} - \alpha_1\nu\kappa^{2/3}A_{1,0}\cos\theta_{1,0}, \\ 0 &= A_{n,m}, \quad (n,m) \neq (1,0) \text{ or } (0,1). \end{aligned}\right\} \qquad (2.27)$$

Finally, noting that the leading-order velocity potential is now

$$\phi \sim 2\varepsilon^{1/2}[A_{1,0}\cos x\sin(t + \theta_{1,0}) + A_{0,1}\cos y\sin(t + \theta_{0,1})],$$

we see that (2.27) matches (2.25) if we write $2A_{1,0} = A^*$, $2A_{0,1} = B^*$, $\theta_{1,0} = \theta_1$ and $\theta_{0,1} = \theta_2$.

In this section we have presented a framework for two-dimensional oscillations in the simplest parameter regime $\nu_0 = O(\varepsilon^{1/2})$ where the detuning, geometrical effects and nonlinearity balance when second-order terms are considered. We have found that the degeneracy induced by the condition $h_0/L = \pi$ causes the response in the cross-direction to be much stronger than in non-degenerate cases. This phenomenon had already been noticed for deep water in (1.13), with which the results of this section are consistent. However, as was the case for the thin resonators considered in Ockendon *et al.* (1993), we can make certain less precise statements about the regime $1 \gg \nu_0 \gg \varepsilon^{1/2}$ and this is one of the generalizations we consider in the next section.

3. Generalizations

3.1. *Stronger geometric variations*

Having established a basic theoretical framework for the regime $\nu_0 = O(\varepsilon^{1/2})$, we could attempt to bridge the gap to the regime $\nu_0 = O(1)$, where we almost always expect a single mode response, in the same spirit as described for thin resonators at the end of §1.3. Indeed the similarities that have emerged between the effects of increasing geometric imperfections in thin resonators and in nearly square resonators for the case $\nu_0 = O(\varepsilon^{1/2})$ suggest that some of the arguments of Ockendon *et al.* (1993) could also

apply to the progressive destruction of degeneracy as v_0 increases. However, it soon becomes apparent that the details are even more intricate than those mentioned in Ockendon *et al.* (1993) so we will restrict ourselves to some very general observations here.

Let us now consider what happens when $v_0 \gg \varepsilon^{1/2}$. The simplest regime where this holds is when $v_0 \sim O(\varepsilon^{1/4})$ and in this case we proceed as in §1.3.2, but now expand φ as $\varphi \sim \varepsilon^{-1/2}\varphi_0 + \varepsilon^{-1/4}\varphi_1 + \varphi_2 + \cdots$, where φ_0 still satisfies (1.15) and hence can be written as (2.2). However, at second order, we now find that the $f_{n,m}$ must be such that

$$\frac{1}{\pi^2}\sum_{p=1}^{\infty}\int_0^{2\pi}\int_0^{\pi} R(x,t')(-1)^{pm}\cos pnx\cos p\lambda_{n,m}(t'-t)\mathrm{d}x\,\mathrm{d}t' = \frac{2\alpha_0 m^2}{\lambda_{n,m}^2}f''_{n,m}, \qquad (3.1)$$

for all (n,m), for periodic solutions to be possible. When we consider this set of conditions by writing the $f_{n,m}$ and $a(x)$ as Fourier series, we find an infinite set of restrictions on the coefficients of these series which will, in general, force all the $f_{n,m}$ to vanish to lowest order and thus rule out any anomalous large-amplitude response over and above a single mode with a dimensional amplitude of $O(\varepsilon^{3/4}\omega L^2)$. However, there may be exceptions when the α_i obey certain very special conditions. This can best be seen by assuming the perturbations to the natural frequencies caused by the back variations are such that

$$\omega_{n,m} = (n^2+m^2)^{1/2}\left[1 + v_0\begin{Bmatrix}\omega^+_{(n,m)1}(\alpha_i)\\ \omega^-_{(n,m)1}(\alpha_i)\end{Bmatrix} + v_0^2\begin{Bmatrix}\omega^+_{(n,m)2}(\alpha_i)\\ \omega^-_{(n,m)2}(\alpha_i)\end{Bmatrix} + O(v_0^3)\right],$$

as $v_0 \to 0$, where n^2+m^2 is the square of an integer, $\pm$ denotes the split of the natural frequencies due to the degeneracy and $\omega^{\pm}_{(n,m)j}$ are functions of the Fourier coefficients α_i. For the case considered in §2, when $v_0 \sim O(\varepsilon^{1/2})$, we find that the detuning $\lambda_0 \sim O(\varepsilon^{1/2})$ balances with the $v_0\omega^{\pm}_{(n,m)1}$ terms along spectral lines such as (2.18) and this balance is associated with the sub-resonant growth of the associated modes. Now, for the regime considered here ($v_0 \sim O(\varepsilon^{1/4})$), the detuning will only balance with the $v_0^2\omega^{\pm}_{(n,m)2}$ terms and these sub-resonances will only be possible if the corresponding $v_0\omega^{\pm}_{(n,m)1}$ vanish (i.e. when the α_i satisfy certain constraints). Thus, unless all the $\omega^{\pm}_{(n,m)1}$ vanish, (3.1) will mean that some of the modes in the $f_{n,m}$ must also vanish. Note that these special cases, where large-amplitude responses occur, do not correspond to the extension of the fingers found in §2 but are associated with the emergence of these fingers much further up the v_0-axis as illustrated in the shock diagram figure 9. If $\omega^{\pm}_{(n,m)1}$ do not vanish, we are effectively far from resonance with $\varphi_0 = 0$ and $\varphi \sim O(\varepsilon^{-1/4})$.

We note also that the emergence of these special large-amplitude responses is critically dependent on α_0. For $\alpha_0 \neq 0$, we find that (3.1) are only satisfied when $f_{n,m} = 0$, $(n,m) \neq (1,0)$, and $f_{1,0}$ may contain a number of modes depending on the other α_i as in Ockendon *et al.* (1993). For $\alpha_0 = 0$, however, it is possible to find a response containing a number of modes in wavetrains other than the longitudinal wavetrain just as long as the other α_i are suitably chosen. This difference can be seen by recalling that $v_0\alpha_0$ is the average of the back variation and, whenever this quantity is greater than $O(\varepsilon^{1/2})$, we are sufficiently removed from the degenerate case of a square tank that, to leading order, we have a one-dimensional response.

When we finally attain the regime $v_0 \sim O(1)$, we can see that a generalization of the above arguments suggests that there will only be a non-trivial response when the

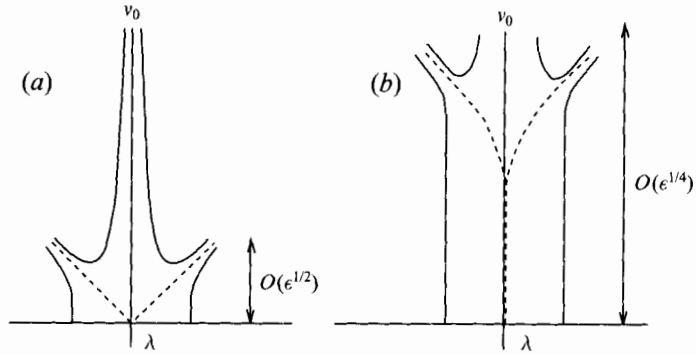

FIGURE 9. Shock diagrams showing subresonant growth of the first mode in the $f_{1,0}$ and $f_{0,1}$ wavetrains along fingers in the detuning range $\lambda_0 \sim O(\epsilon^{1/2})$: (*a*) $v_0 \sim O(\epsilon^{1/2})$, where the detuning balances with $v_0\omega^{\pm}_{(1,0)1}$; (*b*) $v_0 \sim O(\epsilon^{1/4})$, where the detuning balances with $v_0^2\omega^{\pm}_{(1,0)2}$ and $\omega^{\pm}_{(1,0)1} = 0$. In both cases the dashed line indicates the spectral lines.

distance of the $\omega_{n,m}$ from a commensurate set is $O(\epsilon^{1/2})$ and this will require a very special geometry.

3.2. *Spectra with other degeneracies*

The discussions in §2 and §3.1 have been solely concerned with the two-dimensional response of a nearly square resonator, so that the eigenvalues are nearly $n^2 + m^2$ and all are nearly degenerate. We can destroy many of these degeneracies by the artifice of introducing three-dimensionality and putting a slightly uneven 'lid' $z = d_0(1+\beta h(y))/L$ on the resonator. Then, for $d_0/L \ll \epsilon^{1/4}$ and $\beta \sim O(1)$, we can adapt the analysis of Ockendon *et al.* (1993) to find a quasi-two-dimensional problem for the velocity potential $\varphi(x, y, t) \sim \epsilon^{-1/2}\varphi_0 + \varphi_1 + \cdots$,

$$\left.\begin{aligned} \varphi_{0xx} + \varphi_{0yy} + \frac{\beta h'}{1+\beta h}\varphi_{0y} &= \varphi_{0tt}, \\ \varphi_{0x} = 0 \quad \text{on} \quad x = 0, \pi \quad , \quad \varphi_{0y} &= 0 \quad \text{on} \quad y = 0, \pi, \end{aligned}\right\} \tag{3.2}$$

and

$$\varphi_{1xx} + \varphi_{1yy} + \frac{\beta h'}{1+\beta h}\varphi_{1y} = \varphi_{1tt} + \lambda\varphi_{0tt} + 2\varphi_{0x}\phi_{0xt} + 2\varphi_{0y}\varphi_{0yt} + (\gamma - 1)\varphi_{0t}\varphi_{0tt}, \tag{3.3a}$$

$$\varphi_{1x} = 0 \quad \text{on} \quad x = 0, \tag{3.3b}$$

$$\varphi_{1x} = \sin t \quad \text{on} \quad x = \pi, \tag{3.3c}$$

$$\varphi_{1y} = 0 \quad \text{on} \quad y = 0, \tag{3.3d}$$

$$\varphi_{1y} = v\pi[\varphi_{0x}a'(x) - \varphi_{0yy}a(x)] \quad \text{on} \quad y = \pi. \tag{3.3e}$$

The eigenvalues $\omega_{n,m}$ now satisfy the eigenvalue problem

$$\frac{\mathrm{d}}{\mathrm{d}y}\left([1+\beta h(y)]\frac{\mathrm{d}g_{n,m}}{\mathrm{d}y}\right) + [1+\beta h(y)](\omega_{n,m}^2 - n^2)g_{n,m} = 0,$$

$$g'_{n,m} = 0 \quad \text{on} \quad y = 0, \pi,$$

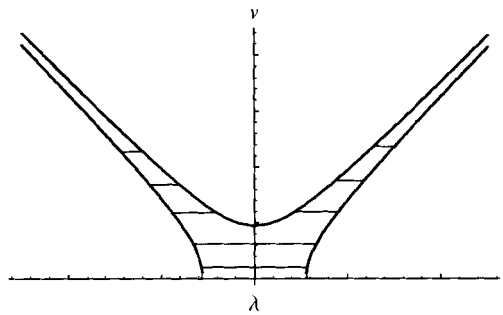

FIGURE 10. Shock diagram for the special case of one transverse mode.

with corresponding solution

$$\varphi_0 = f_{1,0}(t \pm x) + \sum_{n=0}^{\infty}\sum_{m=1}^{\infty} g_{n,m}(y)\cos nx(c_{n,m}\sin\omega_{n,m}t + d_{n,m}\cos\omega_{n,m}t), \tag{3.4}$$

and, as usual, we have written

$$f_{1,0}(\tau) = \tfrac{1}{2}\sum_{n}(a_{n,0}\cos n\tau + b_{n,0}\sin n\tau).$$

Now let us suppose we can select an $h(y)$ such that $\omega_{0,1} = 1$ and no other $\omega_{n,m}$ $(n \neq 0)$ is commensurate with it.† Then we only need $n = 0, m = 1$ in the summation in (3.4) and the application of the Fredholm Alternative to (3.3) gives

$$\lambda f''_{1,0} + (\gamma+1)f'_{1,0}f''_{1,0} = -\frac{\sin t}{\pi} - \frac{\pi g_1 g''_{0,1}(\pi)\alpha_1 v}{2}(c_{1,0}\cos t + d_{1,0}\sin t) + \frac{g_1 v}{2}\int_0^{\pi} f'_{1,0}(2x+t)[a'(x) - a'(\pi - x)]\mathrm{d}x, \tag{3.5a}$$

$$\begin{Bmatrix} c_{0,1} \\ d_{0,1} \end{Bmatrix} = -\frac{\pi v\alpha_1 g_2}{2(\lambda - g_2 g''_{0,1}(\pi)\pi\alpha_0 v)}\begin{Bmatrix} a_{1,0} \\ b_{1,0} \end{Bmatrix}, \tag{3.5b}$$

where

$$g_1 = \frac{1+\beta h(\pi)}{\displaystyle\int_0^{\pi}[1+\beta h(y)]\mathrm{d}y}, \quad g_2 = \frac{g_{0,1}(\pi)[1+\beta h(\pi)]}{\displaystyle\int_0^{\pi} g_{0,1}^2(y)[1+\beta h(y)]\mathrm{d}y}.$$

We can only easily see what happens in the symmetric case $a'(x) = a'(\pi - x)$ and we first consider the case $\alpha_0 = 0$. Then (3.5a) has discontinuous solutions for

$$\lambda^2 \leqslant \frac{16(\gamma+1)}{\pi^3}\left[-\frac{\pi^3\alpha_1^2 g_1 g_2 g''_{0,1}(\pi)v^2}{6(\gamma+1)} \pm 1\right], \tag{3.6}$$

and we plot the shock regime in the shock diagram in figure 10. Equations (3.5) reveal three different classes of behaviour depending on the parameter λ/v^2. First, when $v^2 \ll \lambda$, the geometric imperfection in the rear wall is so weak that $c_{0,1}$ and $d_{0,1}$ are negligible and we return to the one-dimensional response. Also, when $v^2 \sim \lambda$, the primary and transverse wavetrains are both of the same order of magnitude as in

† Using a numerical method (Nag Fortran Library 1990) we found that $1 + \beta h(y) = [\cos(1.04y + 3)]^{-1}$ yields $\omega_{n,m} = 1$ for the case $n = 0$ with the next few $\omega_{n,m}$ being non-commensurate and hence a function of this general shape may be a suitable example.

the case $v = O(1)$ in §2. However, we have an interesting anomalous response when $v^2 \gg \lambda$, because then $f_{1,0} \sim O(\lambda/v^2)$ and the transverse wavetrain (in the y-direction) dominates. Indeed, from (3.5), we find, in both shock and continuous regions, that

$$a_{1,0} \sim 0 \quad , \quad b_{1,0} \sim -\lambda/v^2 \quad , \quad c_{0,1} \sim 0 \quad , \quad d_{0,1} \sim -1/v,$$

so that, as $\lambda \to 0$, the wavetrain in the x-direction (which may contain a shock) is of $O(\lambda/v)$ lower than the lowest-order transverse wavetrain (which is smooth). This is due to the amplification of the relatively small primary wavetrain resulting from resonance with the rear wall geometry which causes a forcing at a transverse frequency (that is, in turn, dictated by the shape of the 'lid'). Thus, although figure 10 suggests some similarities with the 'fingers' of figures 3 or 6(a), where all the purely transverse modes are commensurate and degenerate, the behaviour near $\lambda = 0$ is very different, with the single transverse mode now dominating for small λ and $v^2 \gg \lambda$; also, of course, the resonant response only ever contains shocks propagating in the primary (x) direction.

For $\alpha_0 \neq 0$, the transverse mode dominates close to the line $\lambda = g_2 g''_{0,1}(\pi)\pi\alpha_0 v$ so that the finger near $\lambda = 0$ is retained in this case. The effect of the transverse mode dominating will be to cause any fingers close to the line $\lambda = g_2 g''_{0,1}(\pi)\pi\alpha_0 v$ to becomes thinner as the longitudinal motion becomes weaker.

We may also remark that if other eigenvalues rather than just the fundamental are degenerate, then, away from $\lambda = 0$, the scenario suggested by figures 3, 6(a) and 10 will persist, with shock fingers spilling out into the shock diagram.

3.3. *The effect of other physical mechanisms*

The principal mechanisms that we have neglected in all our models are dissipation and, in the case of sloshing, surface tension. It is relatively easy to take the latter into account by introducing the terms $\sigma_s \varepsilon^{1/2}[\bar{\eta}_{xx} + \bar{\eta}_{yy}]$ and $\sigma_s A_{tttt}$ into the right-hand sides of (1.18g) and (1.20a) respectively, where σ_s measures surface tension. Thus the zero-dispersion limit merely becomes $\kappa \downarrow \sqrt{3}\sigma_s$ rather than $\kappa \to 0$ and, as long as $\kappa > \sqrt{3}\sigma_s$, i.e. the depth is greater than the ripple depth, all our previous analysis applies qualitatively. Nonlinear effects in sloshing tanks at depths less than the ripple depth do not appear to have been analysed asymptotically.

As far as the effects of dissipation are concerned, we have primarily neglected them thus far on theoretical grounds in order to facilitate our analysis of nonlinear and dispersive phenomena. In practice viscous action will be important in all the problems we have described and we have implicitly acknowledged this in focusing attention only on periodic responses at the driving frequency. The precise mechanism for viscous action will of course vary from problem to problem, but in high Reynolds number situations it will be concentrated in viscous boundary layers on the walls of the tank or resonators. It is much easier to model bulk viscous action than the effect of boundary layers; as demonstrated in Ockendon *et al.* (1986) the introduction of a term $\varepsilon^{2/3}\mu\dot{x}$ into Duffing's equation (1.1) or $\mu f'$ into Chester's equation (1.2) can be handled quite easily and it simply results in a 'round off' of all the response diagrams we have presented. A more realistic model for two-dimensional boundary layer dissipation has been proposed in the form of a linear time convolution by Chester (1964), but this is quite difficult to handle asymptotically, as shown in Chester (1964, 1968), Keller (1976) and Ockendon & Ockendon (1973). Even more difficult is the nonlinear history dependence that would result from taking a full boundary layer model. A further complication in our configuration would be that the dominant boundary layer

action would probably be confined to three-dimensional boundary layers near the edge of the tanks or resonators.

3.4. *Further remarks*

The configurations that have been studied hitherto by no means exhaust the possibilities for multi-dimensional resonant fluid responses. For example, although the case of sloshing tanks of infinite depth is a trivial special case of what we have described earlier, tanks of semi-infinite horizontal extent have continuous spectra and hence offer quite new possibilities when being resonated near a cut-off frequency (Ockendon & Ockendon 1973; Barnard, Mahoney & Pritchard 1977; Kit, Shemer & Miloh 1987; Kantzios & Akylas 1988).

There is also the possibility of three-dimensional motions when 'cross-waves' are excited by parametric resonance (Garrett 1970; Miles 1988; Tsai, Yue & Yip 1990); indeed this instability mechanism would be important in some of the problems listed above in §2 when the wavemaker is oscillated at twice the frequency of a harmonic in the transverse direction. We expect our methodology to apply to such solutions, although preliminary investigations suggest the details will be much more complex than those of §2. Such parametric resonances also occur when a tank is oscillated vertically (Faraday 1831; Ockendon & Ockendon 1973; Miles 1984); in both cases we would expect the nonlinearity to enter the analysis in the same way as proposed for the hybrid "Mathieu-Duffing" equation in Ockendon & Ockendon (1973).

Finally, we have made no explicit mention of fully three-dimensional acoustic resonators, but we see no reason why they should not be described by relatively straightforward generalizations of the asymptotic representations listed here, with, for example, two families of transverse shocks being capable of being excited in a nearly cubical resonator.

4. Conclusions

We have described some of the salient features of the multi-mode response of fluid resonators near their fundamental frequency. We have assumed that the amplitude is limited primarily by nonlinear effects and that dissipation is negligible except in that it filters out responses that are not periodic with the same period as the forcing mechanism.

Usually the response is the familiar one in which the waveform is approximately proportional to the lowest eigenmode, with an amplitude related to the detuning in the same way as for a Duffing oscillator. This is because the effects of geometric asymmetry and dispersion usually engender a non-degenerate and non-commensurate spectrum. However, there are special situations when the spectrum has an infinite number of nearly commensurate eigenfrequencies that can all be excited simultaneously. Normally such a configuration can be modelled by the well-known one-dimensional Chester theory, or its extension to nearly one-dimensional resonators. However, this excludes the interesting case in which the spectrum may be nearly degenerate, for which a nearly square two-dimensional acoustic resonator is the paradigm.

For those anomalous acoustic resonators that we have been able to analyse, our principal result is that as geometric imperfections are increased to move the spectrum further away from commensurability and/or degeneracy, a Duffing-like response becomes more and more likely except in narrow regimes (fingers) in the shock-diagram, i.e. the parameter plane of the imperfection and the detuning. In these

fingers, shocks can often exist, sometimes propagating only in the direction of the external forcing, and sometimes transverse to and even dominating the response in that direction.

We have also been able to include dispersion in the theory and hence relate our acoustic predictions to those for sloshing in horizontally oscillated rectangular tanks. Then the spectrum for shallow water sloshing may be nearly commensurate, so that many one-dimensional modes can respond to the forcing. Nonetheless, for the degenerate case of a rectangular tank of nearly square cross-section, forcing parallel to one pair of vertical walls means that a significant response can occur in the perpendicular direction. This transverse excitation also occurs for deep water when the cross-section is nearly square.

In conjunction with the results of Chester (1994), Ellermeier (1994) and Ockendon *et al.* (1993), our predictions suggest that the phenomenon of 'shock fingers' is common enough to be observable in experiments on gases and possibly shallow liquids, although it may be easier to discern the occurrence of perpendicular wavetrains in nearly square tanks of deep water.

Appendix. Coefficients in (1.13)

$$H(h) = -\tfrac{1}{32}\operatorname{sech}^2 h \operatorname{cosech} h(9 + 15\sinh^2 h - 8\sinh^6 h), \tag{A 1}$$

$$J(h) = \frac{1}{8}\frac{\tilde{J}(h)}{(\sqrt{2}\cosh h \sinh\sqrt{2}h - 4\sinh h\cosh\sqrt{2}h)\sinh h\cosh^3 h}, \tag{A 2}$$

$$K(h) = -\frac{\sinh h + h\operatorname{sech} h}{\pi}\int_0^\pi a(x)\cos x\,\mathrm{d}x, \tag{A 3}$$

$$L(h) = \frac{\sinh h + h\operatorname{sech} h}{\pi}\int_0^\pi a(x)\cos 2x\,\mathrm{d}x, \tag{A 4}$$

$$M(h) = \frac{\sinh h + h\operatorname{sech} h}{\pi}\int_0^\pi a(x)\,\mathrm{d}x, \tag{A 5}$$

$$\begin{aligned}\tilde{J}(h) = {} & -29\sqrt{2}\cosh^5 h\sinh\sqrt{2}h + 52\cosh^4 h\cosh\sqrt{2}h\sinh h \\ & +9\sqrt{2}\cosh^7 h\sinh\sqrt{2}h - 40\cosh\sqrt{2}h\cosh^2 h\sinh h \\ & -20\sinh h\cosh^6 h\cosh\sqrt{2}h + 31\sqrt{2}\sinh\sqrt{2}h\cosh^3 h \\ & +8\cosh\sqrt{2}h\sinh h - 11\sqrt{2}\cosh h\sinh\sqrt{2}h.\end{aligned} \tag{A 6}$$

REFERENCES

BARNARD, B. J. S., MAHONY, J. J. & PRITCHARD, W. G. 1977 The excitation of surface waves near a cut-off frequency. *Phil. Trans. R. Soc. Lond.* A **286**, 87–123.

CAN, N. & ASKAR, A. 1990 Nonlinear elastic surface gravity waves: continuous and discontinuous solutions. *Wave Motion* **12**, 485–495.

CHESTER, W. 1964 Resonant oscillations in closed tubes. *J. Fluid Mech.* **18**, 44–65.

CHESTER, W. 1968 Resonant oscillations of water waves. *Proc. R. Soc. Lond.* A **306**, 5–22.

CHESTER, W. 1991 Acoustic resonance in spherically symmetric waves. *Proc. R. Soc. Lond.* A **434**, 459–463.

CHESTER, W. 1994 Nonlinear resonant oscillations of a gas in a tube of varying cross-section. *Proc. R. Soc. Lond.* A **444**, 591–604.

ELLERMEIER, W. 1994 Acoustic resonance of cylindrically symmetric waves. *Proc. R. Soc. Lond.* A **445**, 181–191.

FARADAY, M. 1831 On a peculiar class of acoustical figures; and on certain forms assumed by groups of particles upon vibrating elastic surfaces *Phil. Trans. R. Soc. Lond.* **121**, 299–340.

GARRETT, C. J. R. 1970 On cross-waves *J. Fluid Mech.* **41**, 837–849.

KANTZIOS, Y. D. & AKYLAS, T. R. 1988 Long nonlinear water waves in a channel near a cut-off frequency. *Stud. Appl. Maths* **78**, 57–72.

KIT, E., SHEMER, L. & MILOH, T. 1987 Experimental and theoretical investigation of nonlinear sloshing waves in a rectangular channel. *J. Fluid Mech.* **181**, 265–291.

KELLER, J. J. 1976 Resonant oscillations in closed tubes: the solution of Chester's equation. *J. Fluid Mech.* **77**, 279–304.

KELLER, J. J. 1977 Nonlinear acoustic resonance in shock tubes with varying cross-sectional area. *Z. Angew. Math. Phys.* **28**, 107–122.

LIEPMANN, H. W. & ROSHKO, A. 1957 *Elements of Gas Dynamics.* Wiley & Sons.

MILES, J. W. 1984 Nonlinear Faraday resonance. *J. Fluid Mech.* **146**, 285–302.

MILES, J. W. 1988 Parametrically excited, standing cross-waves *J. Fluid Mech.* **186**, 119–127.

MOISEYEV, N. N. 1958 On the theory of nonlinear vibrations of a liquid. *Prikl. Mat. Mech.* **22**, 612–621.

NAG *Fortran Library Manual* 1990 Mark 14, Chapter D02.

OCKENDON, J. R. & OCKENDON, H. 1973 Resonant surface waves. *J. Fluid Mech.* **59**, 397–413.

OCKENDON, H., OCKENDON, J. R., CHESTER, W. & PEAKE, M. R. 1993 Geometric effects in resonant gas oscillations. *J. Fluid Mech.* **257**, 201–217.

OCKENDON, J. R., OCKENDON, H. & JOHNSON, A. D. 1986 Resonant sloshing in shallow water. *J. Fluid Mech.* **167**, 465–479.

PEAKE, M. R. 1993 Degeneracy in acoustic resonance. DPhil thesis, Oxford University.

TSAI, W. T., YUE, D. K. P. & YIP, M. K. 1990 Resonantly excited regular and chaotic motions in a rectangular wave tank. *J. Fluid Mech.* **216**, 343–380.

WATERHOUSE, D. D. 1994 Resonant sloshing near a critical depth. *J. Fluid Mech.* **281**, 313–318.

WATERHOUSE, D. D. 1995 Resonant oscillations of gases and liquids in three dimensions. DPhil thesis, Oxford University.